Atlantic ocean ventilation changes across the last deglaciation and their carbon cycle implications

L. Skinner, E. Freeman, D. Hodell, Claire Waelbroeck, N. Vazquez Riveiros, A. Scrivner

Paleoceanography and Paleoclimatology

RESEARCH ARTICLE
10.1029/2020PA004074

Atlantic Ocean Ventilation Changes Across the Last Deglaciation and Their Carbon Cycle Implications

L. C. Skinner[1], E. Freeman[1], D. Hodell[1], C. Waelbroeck[2], N. Vazquez Riveiros[3], and A. E. Scrivner[1]

[1]Godwin Laboratory for Palaeoclimate Research, Department of Earth Sciences, University of Cambridge, Cambridge, UK, [2]Laboratoire d'Océanographie et du Climat: Expérimentation et Approches Numériques, LOCEAN/IPSL, Sorbonne Université-CNRS-IRD-MNHN, Paris, France, [3]Laboratoire Géodynamique et enregistrement Sédimentaire (PDG-REM-GM-LGS), IFREMER, Brest, France

Key Points:

- Increased ventilation ages occurred at all sites during the northern hemisphere stadials Heinrich Stadial 1, and the Younger Dryas
- The entire Atlantic was flushed with well-ventilated waters at the onset of the Bølling-Allerød
- Deglacial CO_2 rise linked to abrupt releases from the Atlantic and more sustained release from the Southern Ocean and/or Pacific

Supporting Information:

- Supporting Information S1
- Table S1
- Table S2
- Table S3
- Table S4
- Table S5

Correspondence to:
L. C. Skinner,
lcs32@cam.ac.uk

Citation:
Skinner, L. C., Freeman, E., Hodell, D., Waelbroeck, C., Vazquez Riveiros, N., & Scrivner, A. E. (2021). Atlantic Ocean ventilation changes across the last deglaciation and their carbon cycle implications. *Paleoceanography and Paleoclimatology*, *36*, e2020PA004074. https://doi.org/10.1029/2020PA004074

Received 30 JUL 2020
Accepted 26 NOV 2020

Abstract Changes in ocean ventilation, controlled by both overturning rates and air-sea gas exchange, are thought to have played a central role in atmospheric CO_2 rise across the last deglaciation. Here, we constrain the nature of Atlantic Ocean ventilation changes over the last deglaciation using radiocarbon and stable carbon isotopes from two depth transects in the Atlantic basin. Our findings broadly cohere with the established pattern of deglacial Atlantic overturning change, and underline the existence of active northern sourced deep-water export at the Last Glacial Maximum (LGM). We find that the western Atlantic was less affected by incursions of southern-sourced deep water, as compared to the eastern Atlantic, despite both sides of the basin being strongly influenced by the air-sea equilibration of both northern and southern deep-water end-members. Ventilation at least as strong as modern is observed throughout the Atlantic during the Bølling-Allerød (BA), implying a "flushing" of the entire Atlantic water column that we attribute to the combined effects of Atlantic meridional overturning circulation (AMOC) reinvigoration and increased air-sea equilibration of southern sourced deep-water. This ventilation "overshoot" may have counteracted a natural atmospheric CO_2 decline during interstadial conditions, helping to make the BA a "point of no return" in the deglacial process. While the collected data emphasize a predominantly indirect AMOC contribution to deglacial atmospheric CO_2 rise, via far field impacts on convection in the Southern Ocean and/or North Pacific during Heinrich Stadial 1 and the Younger Dryas, the potential role of the AMOC in centennial CO_2 pulses emerges as an important target for future work.

1. Introduction

Over the last deglaciation, the Atlantic Ocean circulation transitioned from a glacial state with shoaled North Atlantic Deep Water (NADW) (e.g., Adkins, 2013; Bradtmiller et al., 2014; Curry & Oppo, 2005; Freeman, Skinner, Waelbroeck, et al., 2016; Lippold et al., 2012) to the modern, interglacial state with a strong and deep NADW production. During this transition a series of abrupt, millennial-scale climate events occurred (e.g., Blunier & Brook, 2001; Clark et al., 2002; Sarnthein et al., 1994). These events are thought to be linked to perturbations of the Atlantic Ocean circulation that have been identified in numerous records (e.g., Gherardi et al., 2005; McManus et al., 2004; Ng et al., 2018; Piotrowski et al., 2004; Skinner and Shackleton, 2004), and which may have played an active role in the deglacial process (Cheng et al., 2009; Denton et al., 2010; Wolff et al., 2009). Two millennial-scale northern hemisphere stadials are recorded during the last deglaciation, Heinrich Stadial 1 (HS1) and the Younger Dryas (YD) (Björck et al., 1998). These are separated by a relatively warm period in the northern hemisphere, the Bølling-Allerød (B/A), which is synchronous with a cooling in the southern hemisphere, the Antarctic Cold Reversal (ACR) (Björck et al., 1998; Blunier & Brook, 2001). During these periods the Atlantic Ocean circulation may well have been different from both that of the Last Glacial Maximum (LGM) and that of the modern ocean (e.g., Gherardi et al., 2005; Gherardi et al., 2009; McManus et al., 2004; Ng et al., 2018; Roberts et al., 2010; Thiagarajan et al., 2014).

The Atlantic meridional overturning circulation (AMOC) is thought to have been significantly reduced during HS1 and the YD as a result of freshwater input in the North Atlantic that prevented waters becoming dense enough to form deep waters (e.g., Clark et al., 2002; Ganopolski & Rahmstorf, 2001; McManus et al., 2004; Piotrowski et al., 2012), though other triggering mechanisms are also possible (e.g., Dokken

Table 1
Core Locations

Core name	Latitude	Longitude	Water depth
GS07-150-20/2GC-A	04°15.67′S	37°08.24′W	700
GS07-150-17/1GC-A	04°12.98′S	37°04.52′W	1,000
MD09-3257	04°14.68′S	36°21.16′W	2,344
MD09-3256Q	03°32.81′S	35°23.11′W	3,537
JC89-SHAK10-10K	37°50.00′N	09°30.65′W	1,127
JC89-SHAK14-4G	37°50.16′N	09°43.61′W	2,063
JC89-SHAK06-4K	37°33.68′N	10°21.89′W	2,642
MD99-2334K	37°48.07′N	10°10.28′W	3,146
JC89-SHAK03-6K	37°42.54′N	10°29.56′W	3,735
JC89-SHAK05-3K	37°36.26′N	10°41.50′W	4,670

et al., 2013). A reduction in the AMOC would have reduced the heat transport to the North Atlantic, while causing a warming in the southern hemisphere (Ganopolski & Rahmstorf, 2001; Schmittner et al., 2003; Seidov & Maslin, 2001). The B/A warming in the northern hemisphere has been linked to an abrupt intensification of the AMOC (Barker et al., 2009; McManus et al., 2004; Muscheler et al., 2004; Skinner and Shackleton, 2004; Thiagarajan et al., 2014), which may have penetrated particularly deeply into the Southern Ocean (Barker et al., 2009; Skinner et al., 2013; Waelbroeck et al., 2011).

During these northern hemisphere stadials, the atmospheric CO_2 level ($CO_{2\text{-atm}}$) rose gradually, albeit with more abrupt increases at the end of each stadial (~14.8 and 11.7 kyrs BP), as well as in the middle of HS1 (~16.3 kyrs BP) (Marcott et al., 2014; Monnin et al., 2001). During these more abrupt increases, $CO_{2\text{-atm}}$ rose by 10–15 ppm in just 100–200 years (Marcott et al., 2014). The rapidity of these $CO_{2\text{-atm}}$ "jumps" would be consistent with a release of CO_2 from the ocean (Chen et al., 2015), though terrestrial carbon release has also been proposed (Köhler et al., 2014). Atmospheric radiocarbon activity ($\Delta^{14}C_{atm}$) fell during each deglacial North Atlantic stadial and associated gradual pCO_2 increase (Reimer et al., 2013), suggestive of a radiocarbon-depleted source of CO_2, such as the deep ocean (e.g., Burke & Robinson, 2012; Skinner et al., 2010). However, it is possible that anomalies in $CO_{2\text{-atm}}$ and $\Delta^{14}C_{atm}$ did not maintain a constant link during the last deglaciation (Hain et al., 2014). Thus, centennial/millennial $\Delta^{14}C_{atm}$ changes may have been dominated by variations in the rate and extent of NADW formation, which had only a minor direct impact on atmospheric pCO_2 (Hain et al., 2014), but which nonetheless were temporally linked to changes in deep ocean ventilation via the Southern Ocean (Anderson et al., 2009; Skinner et al., 2013; Skinner et al., 2014) that had a much stronger, if also slower, impact on $CO_{2\text{-atm}}$ (Hain et al., 2014; Kohler et al., 2005). The possible role of AMOC variability in $CO_{2\text{-atm}}$ rise across the last deglaciation is further complicated by the suggestion of countervailing impacts during HS1 in particular, when an inferred increase in the respired carbon budget of the intermediate- and deep Atlantic (Lacerra et al., 2017; Schmittner & Lund, 2015) would have acted against any deglacial redistribution of carbon from the ocean interior to the atmosphere, as inferred from, for example, carbonate-ion saturation reconstructions (Yu et al., 2010).

While deglacial changes in $CO_{2\text{-atm}}$ and $\Delta^{14}C_{atm}$ are both likely to be influenced in some way by changes in the ocean circulation over the last deglaciation, many questions remain concerning how and where carbon was released from the ocean, as well as the respective roles of the North and South Atlantic for example. The lack of a more complete understanding of the key deglacial processes is, in part, due to the scarcity of well resolved deglacial records of paleoceanographic proxies, combined with inherent ambiguities associated with each proxy. Despite their potential to provide vital information on both the pattern and the rate of overturning circulation, high resolution radiocarbon-ventilation records, in particular, are lacking in much of the Atlantic Ocean over the deglaciation.

Here, we present a series of new radiocarbon-based ventilation ages for a suite of cores on the Brazil Margin and the Iberian Margin to investigate changes in the distribution of radiocarbon in the Atlantic Ocean at key time intervals over the last deglaciation. These are combined with stable carbon isotope data to help infer changes in the Atlantic Ocean circulation and the impact they had on the carbon cycle.

2. Materials and Methods

2.1. Radiocarbon and Stable Carbon Measurements

Radiocarbon measurements were obtained for benthic and planktonic foraminifera from a suite of sediment cores from the Iberian Margin and the Brazil Margin (Figure 1; Table 1). Stable carbon isotopes were measured on *Cibicidoides wuellerstorfi* from the same samples, where possible. No stable isotope data were measured in SHAK10-10K due to a lack of *C. wuellerstorfi*. Data for core GS07-150-17/1GCA are from Freeman et al. (2015), and for core MD99-2334K from (Skinner et al., 2014). Published stable carbon isotope

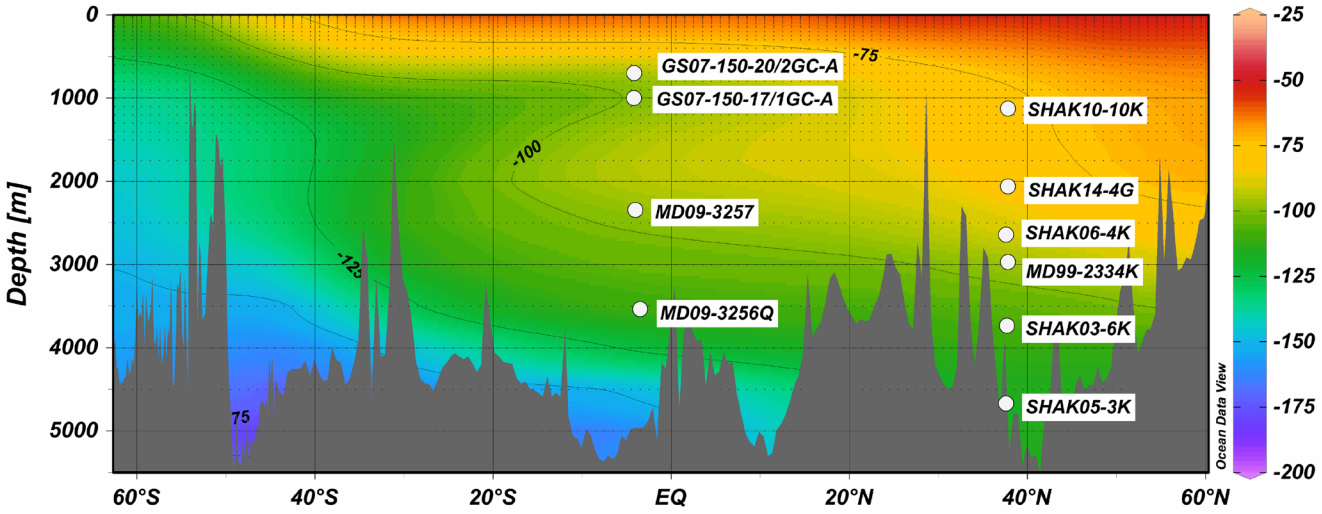

Figure 1. Map of core locations on modern background (GLODAP) $\Delta^{14}C$ (Key et al., 2004).

data from core MD09-3257 (Waelbroeck et al., 2018) are supplemented here by additional measurements. The sediment age models and surface reservoir ages that apply to each of these cores have been updated as described below.

Foraminifera were picked from the >212 μm size fraction and where necessary, from the 150–212 μm fraction. Monospecific samples of planktonic foraminifera, *Globigerinoides ruber* (Brazil Margin) or *Globigerina bulloides* (Iberian Margin), and samples of mixed benthic foraminifera (excluding agglutinated species) were picked and graphitized in the Godwin Radiocarbon Laboratory at the University of Cambridge. Samples were graphitized using a standard hydrogen/iron catalyst reduction method (Freeman, Skinner, Reimer, et al., 2016; Vogel et al., 1984). AMS-^{14}C dates were measured at the 14Chrono Centre, Queens University Belfast. All dates are reported as conventional radiocarbon ages following (Stuiver & Polach, 1977).

Stable carbon isotope measurements were conducted in the Godwin Laboratory, University of Cambridge. Each measurement was run on 1–4 individuals with a combined mass of 50–180 μg. Samples were reacted with orthophosphoric acid (100%) and analyzed, in comparison with a reference gas, using a dual inlet Thermo MAT 253 mass spectrometer connected to a Kiel device. For sediment core MD09-2356Q, stable carbon isotope measurements were also performed at the LSCE in Gif-sur-Yvette (France), on Finnigan Δ+ and Elementar Isoprime mass spectrometers. All results are reported with reference to the international standard VPDB, as $\delta^{13}C$, with a precision better than ±0.06 ‰.

2.2. Chronologies

Calendar age models were constructed for all sediment cores through a multistage process (Skinner et al., 2010; Skinner et al., 2014). The first step in this process consisted of: (1) using chronostratigraphic alignments in "master cores" from each region to provide calendar age constraints for a set of tie-points; (2) transferring these calendar age constraints to other sediment cores in each region, via stratigraphic alignments between the sediment cores; and (3) combining calendar age constraints with radiocarbon dates in each core (interpolating the latter where necessary, as these are generally available at higher resolution than the calendar age pins) to infer surface "reservoir age offsets," which apply exclusively where calendar ages are directly constrained. At this stage, the amplitude and regional consistency of the inferred reservoir age variability was assessed. If reservoir ages were found to differ significantly from the "passive ocean" response that is expected due to changes in atmospheric pCO_2 (Galbraith et al., 2015), then sediment age-depth models were constructed using a regional radiocarbon calibration that takes into account the average reservoir age variability in the region (Skinner et al., 2019), using the *Bchron* age-depth modeling package (Parnell et al., 2008). This was the situation for Iberian Margin cores (see Figure 3b), as has been inferred previously (Freeman, Skinner, Waelbroeck, et al., 2016; Skinner

et al., 2014). If reservoir ages were found to vary broadly as expected from pCO_2 effects, then a radiocarbon calibration based on the "passive ocean" response modeled by (Butzin et al., 2017) was incorporated into *Bchron* instead. This was the case for the Brazil Margin cores (see Figure 4b), in line with the approach taken by Waelbroeck et al. (2019).

Initial calendar age constraints for the Brazil Margin cores were derived by alignment of XRF measurements in MD09-3257 (as an indicator of terrigenous clastic supply (Burckel et al., 2015)) to the high-resolution NGRIP dust record (Ruth et al., 2003) on the GICC05 age-scale (Svensson et al., 2008) (Figure S1). This strategy is supported by the co-occurrence of Greenland stadials with dry periods in Brazil, as recorded in U-series dated δ18O records from the El Condor and Cueva del Diamante speleothems (Cheng et al., 2013). The resulting calendar age "pins" were then transferred to the other Brazil Margin sediment cores, via an alignment of their respective XRF records (Figure S2). For the Iberian Margin cores, initial calendar age constraints were obtained by aligning sedimentary CaCO3%, and planktonic stable oxygen isotopes, in the "master core" MD99-2334K (Skinner et al., 2014), to the event stratigraphies recorded in the Hulu speleothem (Southon et al., 2012) and the NGRIP dust record (Ruth et al., 2003), respectively. We propose that these archives provide valuable age constraints for the middle- (Skinner et al., 2014) and onset of HS1 (Missiaen et al., 2019) (Figure S3). The resulting age constraints were transferred to all other sediment cores from the Iberian Margin via an alignment of high resolution XRF data (Freeman, Skinner, Waelbroeck, et al., 2016) (Figure S4). This transfer of calendar ages was done for the purpose of calculating the surface reservoir ages that are implied by the chronostratigraphic alignment of each sediment core. As noted above, the resulting surface reservoir ages were then used to correct planktonic radiocarbon dates in each core, and thereby generate calibrated radiocarbon chronologies (and associated uncertainties) using *Bchron* (see Figures S5 and S6).

Simpler approaches to the development of chronologies are possible, but come with identifiable drawbacks. First, the simple assumption of invariant reservoir ages must be defended through reference to independent age constraints wherever possible; here, we again confirm that the assumption of invariant reservoir ages on the Iberian Margin (e.g., Stern & Lisiecki, 2013), which experienced ice-rafted debris deposition and significant meltwater supply during Heinrich events (e.g., de Abreu, 2000; Martrat et al., 2007; Skinner et al., 2003; Skinner and Shackleton, 2006), is not supported. Second, while the more direct approach of producing calendar age models from (necessarily) sparse calendar age tie-points (perhaps using a sophisticated, for example, Bayesian, interpolation scheme) may be entirely appropriate in many contexts, it can have the effect of producing reservoir age anomalies where the only constraint on calendar ages is provided by the assumption of approximately constant sedimentation rates (e.g., Umling & Thunell, 2017). Although it can be defended, this approach might not be ideal in a study focusing on marine radiocarbon disequilibria, where we might instead opt to only infer minima/maxima in reservoir ages (and therefore in deep-water radiocarbon ventilation ages) where we have direct chronostratigraphic constraints on the calendar age of radiocarbon dates.

Finally, it is important to note that the final chronologies for the sediment cores do not rely directly on precise claims regarding the stratigraphic alignments, as these are only used to assess surface reservoir age variability in each region. For the Brazil Margin cores, the stratigraphic alignments are not used at all for the final chronologies, which instead derive from calibrated radiocarbon dates, as performed by Waelbroeck et al. (2019). For the Iberian Margin cores, a uniform uncertainty of 200 years is applied to all tie-point calendar ages, which is propagated to the reservoir age estimates using *Radcal* (Soulet, 2015) (see Figure 3b). Only the median reservoir age values provided by *Radcal* are interpolated down-core and used to generate sediment age-depth models using *Bchron* (i.e., without attempting to take into account the R-age and interpolation uncertainties). However, the final uncertainties in the resulting *Bchron* sediment age-depth models readily encompass the plausible level of uncertainty in the initial "target" stratigraphic alignments. This is confirmed by the fact that the initial chronostratigraphic alignments proposed for the "master cores" in each region (MD99-2334K and MD09-3257) are not strictly adhered to by the final *Bchron* chronologies, but do generally lie within the uncertainty limits (see Figures S5 and S6). However, it is notable that adopting a scenario of "minimal" surface reservoir age variability on the Brazil Margin, that is, as modeled by Butzin et al. (2017) and consistent with the approach of Waelbroeck et al. (2019), results in younger calendar ages at what we believe

represents the HS1-BA transition than based on stratigraphic alignment (see Figure 4 and Figure S6). The implications of these age-model differences for radiocarbon ventilation age estimates is illustrated in Figures 3 and 4. Due to the inherent uncertainties (and potential biases) in the age-models, we urge some caution in interpreting the centennial-scale timing of proxy changes, in particular near the BA transition on the Brazil Margin. Our final chronologies represent a compromise between hypothetical chronostratigraphic alignments, regional coherence of reservoir age variability, planktonic radiocarbon dating, and possible sedimentation rate variability between dated intervals. This compromise is motivated by the expectation that an "optimal chronology" would fully satisfy all of these constraints at once.

3. Results

3.1. Deglacial Ocean Ventilation on the Iberian Margin and the Brazil Margin

Broadly similar patterns of millennial-scale changes in ventilation are seen on both the Iberian and Brazil margins over the last deglaciation (Figures 2–4), resembling in very general terms the deglacial pattern of AMOC changes reconstructed in the western deep Atlantic (McManus et al., 2004) (Figure 5). As shown previously for these sites (Freeman, Skinner, Waelbroeck, et al., 2016), radiocarbon ventilation ages were significantly higher than modern at the LGM at all sites deeper than 1,000 m, though hardly changed at shallower depths. An increase in radiocarbon ventilation ages is observed at all sites during North Atlantic stadials, HS1 and the YD, though the timing and magnitude of the increases varies from site to site. Notably, locations near ~2,000 m water depth show the largest changes across these millennial events, particularly on the Brazil Margin. In opposition to the anomalies seen during HS1 and the YD, all sites >1,000 m water depth exhibit a strong pulse of ventilation (i.e., reduced radiocarbon ventilation ages) during the B/A interstadial.

3.2. Deglacial Stable Carbon Isotopes

At the LGM, Iberian Margin $\delta^{13}C$ values at 2.1 km were lower than modern but significantly higher (by ~0.6‰) than those of the deep waters below (3.1–4.7 km) (Figure 3). A strong vertical gradient in $\delta^{13}C$ is therefore apparent on the Iberian Margin at the LGM, particularly between 2.1 and 3.1 km water depth (Freeman, Skinner, Waelbroeck, et al., 2016). At the start of the deglaciation (~17.5 kyrs BP) $\delta^{13}C$ values at 2.1 km rapidly decreased and converged with the deep $\delta^{13}C$ values, which changed little and remained low. All four Iberian Margin sites then show a very similar trend over the deglaciation (~17.5–11 kyrs BP) (Figure 3). The lowest $\delta^{13}C$ values occur during HS1 in all four cores, which also exhibit a marked and abrupt shift to high $\delta^{13}C$ values during the B/A. A return to lower $\delta^{13}C$ values is again apparent during the YD at all sites, though this reversal appears to be weaker, and is less well-resolved, in the deeper cores (due to lower sedimentation rates and lower abundances of epibenthic foraminifera).

At the LGM, the shallowest site for which we have data on the Brazil Margin (1 km) exhibits relatively high $\delta^{13}C$ values (>0.8‰) compared to the deepest site (3.5 km), which had an average value of 0.1‰ (Figure 4). A strong vertical gradient in $\delta^{13}C$ is therefore apparent on the Brazil Margin at the LGM, as observed on the Iberian Margin, and as has been noted previously in the Atlantic (Curry & Oppo, 2005; Oppo & Lehman, 1993). During HS1, this gradient is eliminated below ~2,300 m, again as seen on the Iberian Margin. Mid-depth (2.3 km) $\delta^{13}C$ values thus converged with those of deeper waters during HS1 (consistent with previous evidence for a strong negative excursion at mid-depths on the Brazil Margin (Tessin & Lund, 2013)), whereas those at shallow-intermediate depths (1,000 m) remained slightly higher. During the B/A, $\delta^{13}C$ values rapidly returned to high, near-modern values between 1 and 2.3 km, whereas only a small increase occurred at 3.5 km. An abrupt shift to higher $\delta^{13}C$ values is not seen at 3.5 km on the Brazil Margin until the start of the YD, when a shift back to lower values occurs at 1 km and at 2.3 km. All three cores from the Brazil Margin ultimately converge again at near-modern values at the transition from the YD to the Holocene.

4. Discussion

4.1. East-West Divide in AMOC Control of Atlantic Radiocarbon Ventilation

The general pattern of radiocarbon ventilation that is observed on both the Iberian and Brazil Margins is consistent with that suggested by individual coral and foraminifer dates compiled from other locations in northern and equatorial Atlantic (Chen et al., 2015; Robinson et al., 2005) (as well as that previously reported in core MD99-2334K (Skinner and Shackleton, 2004; Skinner et al., 2014)). This general pattern is characterized by negative ventilation anomalies during HS1/YD, and a strong positive ventilation anomaly during the B-A. It broadly resembles the pattern exhibited by changes in AMOC transport reconstructed in the deep western Atlantic (McManus et al., 2004) (Figure 5), consistent with the interpretation of a dominant influence of AMOC anomalies on deglacial Atlantic radiocarbon ventilation change (Keigwin & Schlegel, 2002; Robinson et al., 2005; Skinner and Shackleton, 2004; Skinner et al., 2014; Thornalley et al., 2011). However, differences between the radiocarbon and Pa/Th signals, as well as spatial heterogeneities in the radiocarbon signals, serve to illustrate more precisely the nature of this AMOC influence. Three key observations emerge. The first is that whereas Pa/Th-based AMOC transport reconstructions from the west Atlantic show a distinct but relatively small difference in circulation strength during the LGM as compared to the B-A and the late Holocene (with two strong negative anomalies occurring during HS1 and the YD) (Ng et al., 2018), a similar pattern in B-Atm ventilation ages is only exhibited on the Brazil Margin ~2.5 km water depth (see Figure 5e). While our radiocarbon ventilation record from a similar depth (~2.1 km) on the Iberian Margin is not well resolved enough to constrain a sharp decline in ventilation at the onset of HS1, benthic $\delta^{13}C$ measurements suggest that this location also experienced a strong hydrographic change at this time, as on the Brazil Margin and unlike deeper sites throughout the Atlantic (Figures 3–5). The mid-depth Atlantic, ~2 km, would therefore appear to have experienced the strongest changes in water-mass sourcing and/or transport across the last deglaciation, most likely due to the changing influence of abyssal-versus

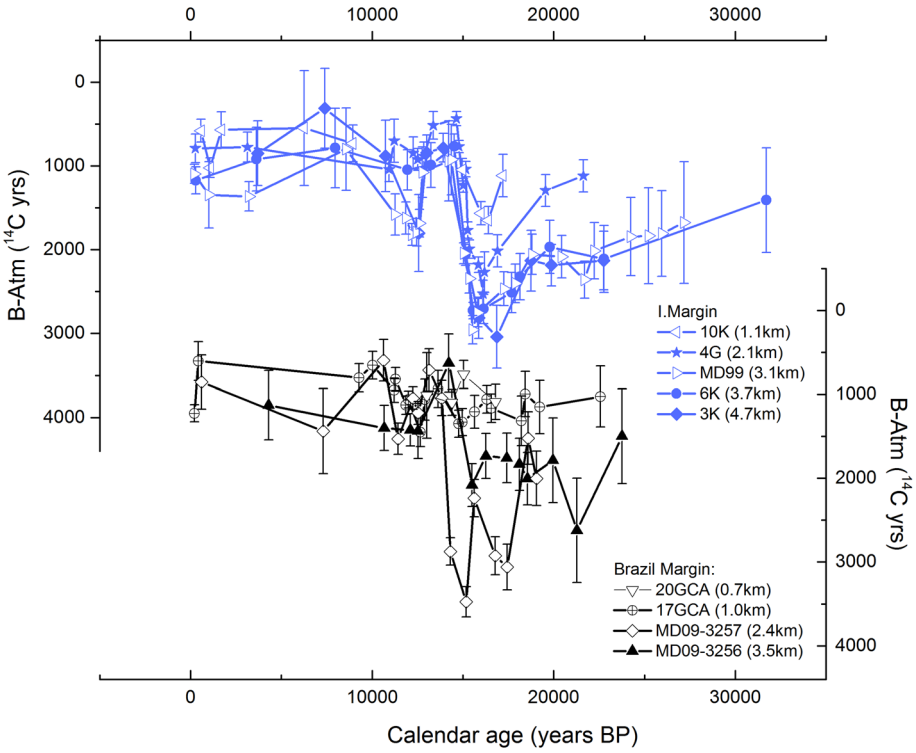

Figure 2. Deglacial deep-water radiocarbon ventilation (B-Atm) records from the Iberian- (upper plot) and Brazil (lower plot) Margins. Error bars correspond to estimates of the 1-sigma uncertainties in B-Atm, derived using Radcal (Soulet, 2015). Note that the B-Atm uncertainties are not independent of calendar age uncertainties, which in turn tend to be correlated in depth, from sample to sample.

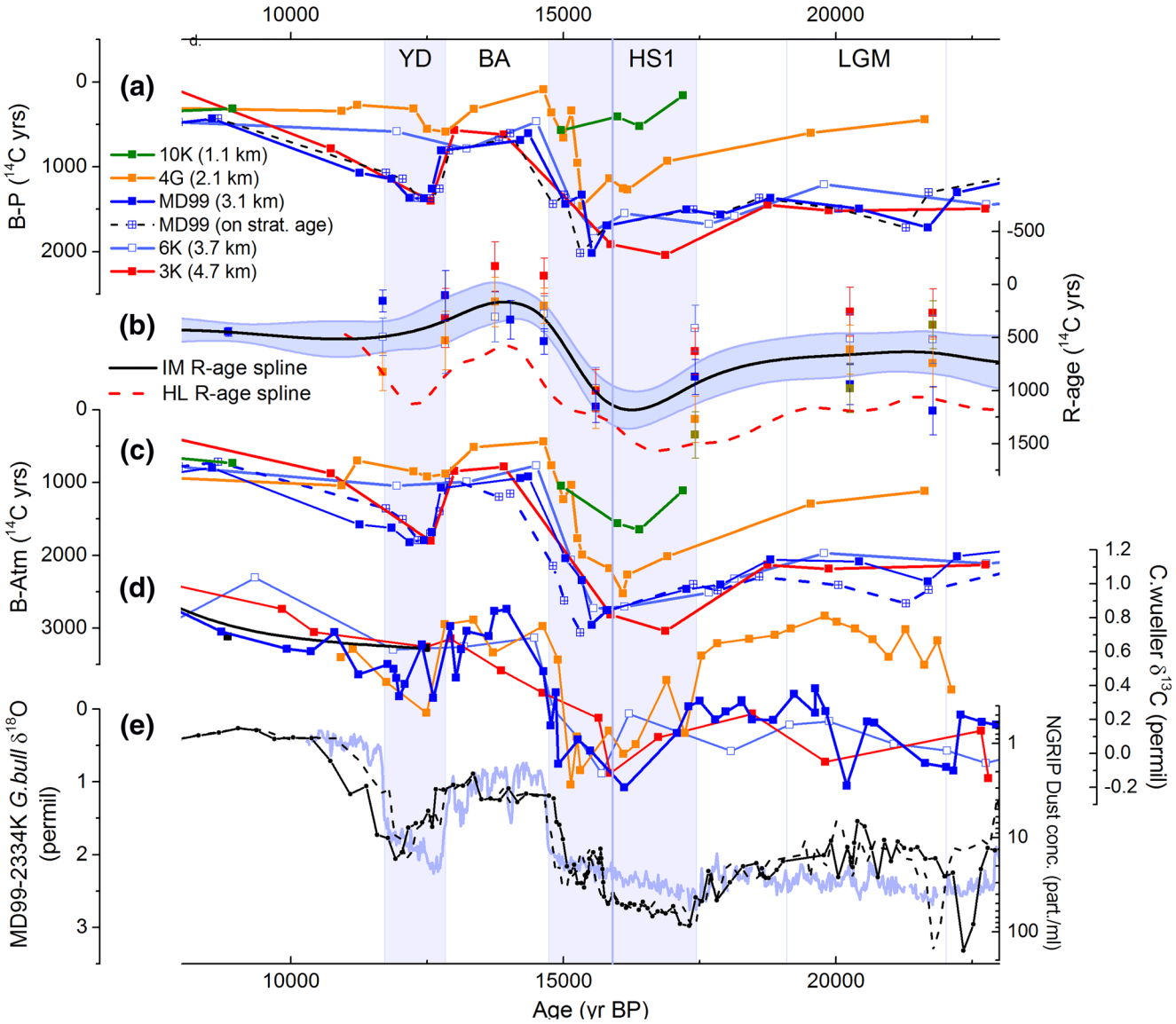

Figure 3. Deglacial records from the Iberian Margin: (a) Benthic-planktonic radiocarbon age offsets. (b) Surface reservoir age estimates for the Iberian Margin sites (symbols as for plot a, with estimated 2-sigma uncertainties), including a best fit cubic spline with 95% confidence intervals (black line and shaded area); the best fit cubic spline for high latitude North Atlantic reservoir ages is shown by the dashed red line (Skinner et al., 2019). (c) B-Atm ventilation ages on the Iberian Margin (symbols as for plot a). (d) Benthic δ^{13}C on the Iberian Margin (symbols as for plot a). (e) Dust concentrations in the NGRIP ice-core, and planktonic d18O from core MD99-2334K, illustrating the chronostratigraphic context, as well as the difference between strict adherence to a stratigraphic age-model (see Figure S3), vs. the calibrated radiocarbon age model that has been adopted. Vertical shaded bars show the northern hemisphere stadials, HS1, and the YD; vertical lines indicate the boundaries of the LGM and the timing of the abrupt jump in CO_2 observed in the WAIS Divide ice core at ~16.3 ka BP. HS1, Heinrich Stadial 1; LGM, Last Glacial Maximum; YD, Younger Dryas.

intermediate water masses, but perhaps also with an influence from enhanced accumulation of respired organic carbon due to slower transport times (Lacerra et al., 2017; Schmittner & Lund, 2015).

A second key observation is that radiocarbon ventilation records from the shallow intermediate- (~1 km) and deepest (>3 km) western Atlantic (i.e., above and below ~2 km) show relatively muted radiocarbon ventilation changes, which hardly differ from those inferred for the high-latitude North Atlantic surface ocean (Skinner et al., 2019) (Figure 5c). This implies that radiocarbon ventilation records from the western/shallow Atlantic do not primarily reflect transport changes between the LGM and the late Holocene (which may have been too subtle to impact significantly on radiocarbon ventilation ages), except near ~2 km water depth perhaps. Arguments for an active overturning cell in the Atlantic during the LGM and HS1 have

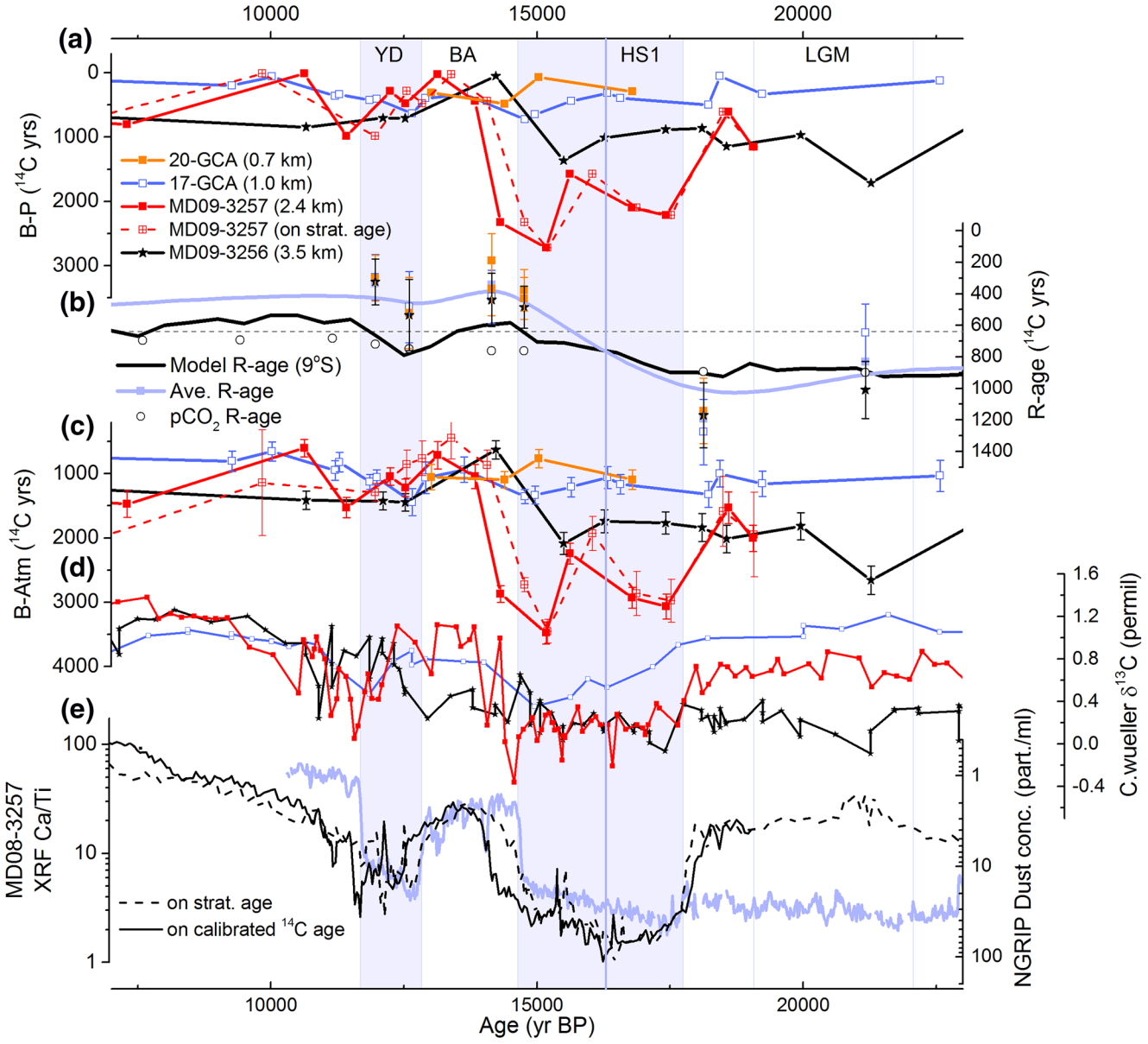

Figure 4. Deglacial records from the Brazil Margin: (a) Benthic-planktonic radiocarbon age offsets. (b) Surface reservoir age estimates for the Brazil Margin sites (symbols as for plot a, with estimated 2-sigma uncertainties, and light blue line), local modern reservoir ages augmented by the effects of atmospheric pCO_2 changes (open circles), and modeled reservoir ages for this locality (black line; Butzin et al., 2017). (c) B-Atm ventilation ages on the Brazil Margin (symbols as for plot a). (d) Benthic $\delta^{13}C$ on the Brazil Margin (symbols as for plot a). (e) Dust concentrations in the NGRIP ice-core, and XRF Ca/Ti in core MD08-3257, illustrating the chronostratigraphic context, as well as the difference between strict adherence to a stratigraphic age-model (see Figure S1), vs. the calibrated radiocarbon age model that has been adopted. Vertical shaded bars show the northern hemisphere stadials, HS1, and the YD; vertical lines indicate the boundaries of the LGM and the timing of the abrupt jump in CO_2 observed in the WAIS Divide ice core at ~16.3 ka BP. HS1, Heinrich Stadial 1; LGM, Last Glacial Maximum; YD, Younger Dryas.

previously been made on the basis of Pa/Th evidence (Böhm et al., 2014; Bradtmiller et al., 2014; Lippold et al., 2012). This situation contrasts with the Iberian Margin, in the eastern North Atlantic, where radiocarbon ventilation ages show larger amplitude changes across the deglaciation, especially >3 km water depth (Figure 5d). This could reflect a more significant influence on radiocarbon ventilation due to the incursion of southern-sourced Lower Deep Water (LDW) (van Aken, 2000) in the eastern Atlantic, both at the LGM (Curry & Lohmann, 1983), and during HS1 (Skinner et al., 2003; Skinner and Shackleton, 2004). This hydrographic geometry, characterized by something of an east-west divide, may have been aided by the continued export of a well-ventilated Northern sourced deep-water mass at the LGM (Keigwin & Swift, 2017; Pöp-

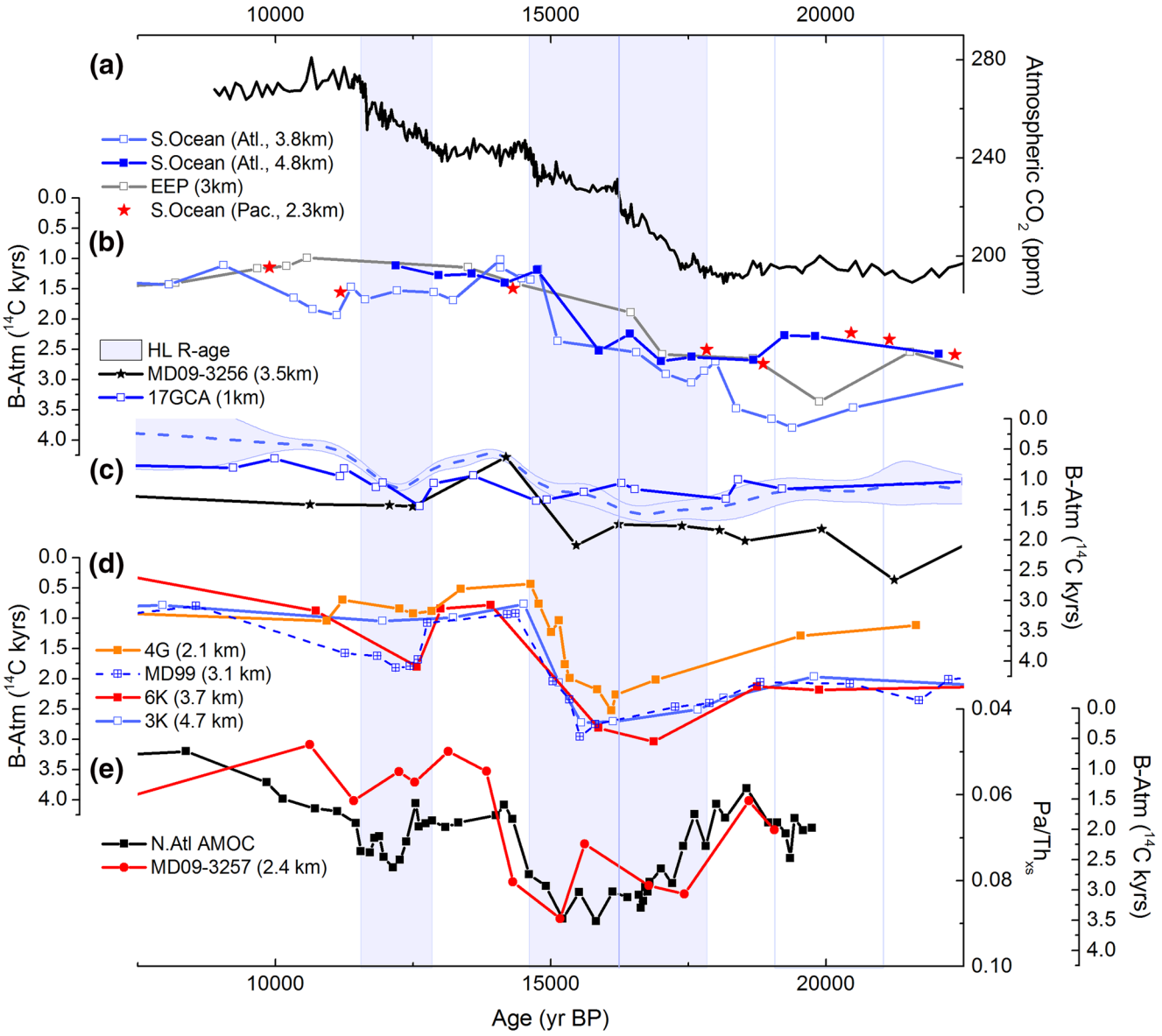

Figure 5. Atlantic radiocarbon ventilation records in context: (a) atmospheric CO_2 concentrations recorded in the WAIS Divide ice core (Marcott et al., 2014); (b) ^{14}C-ventilation records from the deep Southern Ocean and Pacific (blue filled squares and line, deep subtropical Atlantic (Barker et al., 2010; Diz & Barker, 2015); light blue open squares and line, subAntarctic Atlantic (Skinner et al., 2010); gray open squares and line, EEP (de la Fuente et al., 2015); and red stars, deep subAntarctic Pacific (Skinner et al., 2015)); (c) ^{14}C-ventilation records from the western Atlantic basin (black stars and line, this study; blue open squares and line, this study and (Freeman et al., 2015); olive open circles, (Chen et al., 2015); gray crossed squares and line, compiled data from the NW Atlantic (Keigwin & Schlegel, 2002; Robinson et al., 2005)), compared with compiled surface reservoir ages from the high latitude Northeast Atlantic (light blue shaded area and line, Skinner et al., 2019); (d) ^{14}C-ventilation records from the Iberian Margin (symbols as for Figure 2; this study); (e) AMOC variability reconstructed from Pa/Th ratios (black squares and line; McManus et al., 2004), compared with ^{14}C-ventilation records from the Brazil Margin at 2.4 km water depth (red circles and line; this study). Vertical shaded bars show the northern hemisphere stadials, HS1 and the YD; vertical lines indicate the boundaries of the LGM and the timing of the abrupt jump in CO_2 observed in the WAIS Divide ice core at ~16.3 ka BP. HS1, Heinrich Stadial 1; LGM, Last Glacial Maximum; YD, Younger Dryas.

pelmeier et al., 2018), which was blocked from entering the eastern basin by the mid-Atlantic Ridge (Curry & Lohmann, 1983). Here, we emphasize the important influence on radiocarbon ventilation ages throughout the Atlantic due to changing "preformed" radiocarbon signatures, occurring in both the northern and southern high latitudes (Skinner et al., 2019), as well as the additional influence of changing water-mass distribution, which appear to have affected the deep eastern Atlantic more significantly.

Similar considerations are relevant to benthic $\delta^{13}C$ changes. For example, during the YD, $\delta^{13}C$ values decreased at all but the deepest site (3.5 km) on the Brazil Margin (Figure 4). Instead, at the deepest site on the Brazil Margin, $\delta^{13}C$ increased by up to 0.5‰. This increase is unexpected given the parallel increase in radiocarbon ventilation ages. This may reflect an increasing end-member $\delta^{13}C$ for AABW over the deglaciation as suggested by deep South Atlantic records (e.g., Jonkers et al., 2015; Lund et al., 2015; Thiagarajan et al., 2014), potentially as a result of increased air-sea gas exchange (Lynch-Steiglitz et al., 1995). Lower $\delta^{13}C$ values at the other sites, in contrast, may reflect a decrease in the end-member $\delta^{13}C$ value of NADW or may indicate nonconservative behavior of $\delta^{13}C$ (i.e., respired carbon addition). During abrupt climate events, end-member values are hard to identify, adding complexity to the interpretation of hydrographic changes that may not simply represent the varying relative influences of NADW versus AABW in the deep ocean.

A third important observation is that the general pattern of radiocarbon ventilation exhibited across the North Atlantic water column differs from that seen in the deep subAntarctic Atlantic (Skinner et al., 2010), the intermediate-depth Southern Ocean (Burke & Robinson, 2012; Hines et al., 2015), and the deep Pacific (de la Fuente et al., 2015; Skinner et al., 2015) (Figure 5). In contrast to the North Atlantic, these Southern Ocean/Pacific locations tend to show an increase in ventilation from the onset of HS1, and perhaps also (albeit less clearly) during the YD. This has been suggested previously to reflect a "bipolar seesaw" in deep convection operating between the North Atlantic and the Southern Ocean (Skinner et al., 2014), essentially as proposed by Broecker (1998), and consistent with upwelling-driven export productivity pulses observed in the Southern Ocean (Anderson et al., 2009).

Our analysis supports the contention that this "ventilation seesaw" was primarily influenced by surface ocean processes controlling air-sea exchange (Skinner et al., 2019) (e.g., of carbon and heat), augmented by water-mass volume changes that would have modulated the leverage of Southern Ocean gas-exchange on global "disequilibrium carbon" storage (Eggleston & Galbraith, 2018; Galbraith and Skinner, 2020; Ito & Follows, 2013; Skinner, 2009). This is not to say that changes in mass transport did not occur across the last deglaciation (these are well attested to by Pa/Th measurements (McManus et al., 2004; Ng et al., 2018)), but rather that mass transport changes were potentially not the only (or even the primary) influence on the ventilation state of the ocean interior's carbon pool and the re-partitioning of carbon between the ocean and the atmosphere across the last deglaciation (Hain et al., 2014; Khatiwala et al., 2019).

4.2. Insights From Vertical and Lateral Carbon Isotope Gradients

The evolving vertical gradients of radiocarbon ventilation and $\delta^{13}C$ on the Iberian and Brazil Margins provide further insights into the nature of ocean circulation and ventilation changes experienced in the Atlantic across the last deglaciation. Looking first at radiocarbon ventilation gradients across the Atlantic basin, between the Iberian- or Brazil Margins and the Southern Ocean, we find that a positive radiocarbon ventilation gradient (older in the south and younger in the north, as in the modern ocean) is clearly expressed during the LGM and the BA (Figure 6, gray shading). One interpretation of this situation is that it indicates active export of deep-water from the North Atlantic during both the LGM and the BA, without which the gradient would be eliminated or reversed. A collapsed (possibly even reversed) gradient is indeed observed right across the water column during HS1 (Figure 6), consistent with a quasi-elimination of NADW export at this time. A lesser collapse of the meridional ventilation gradient is also observed during the YD (most clearly affecting depths >2,500 m), again consistent with a reduction of NADW export at this time (e.g., Came et al., 2003; Keigwin & Lehmann, 1994; McManus et al., 2004). The meridional gradients in radiocarbon ventilation are therefore consistent with western Atlantic Pa/Th records of AMOC variability (Ng et al., 2018), most notably in suggesting active NADW export at the LGM despite significantly reduced radiocarbon ventilation throughout the deep Atlantic at this time (Freeman, Skinner, Waelbroeck, et al., 2016; Skinner et al., 2017). Although the interpretation of severely restricted NADW export during HS1 might be challenged on the basis that northern and southern end-member radiocarbon signatures may have become very similar (without a change in the export of a northern component), current reconstructions of surface "reservoir ages" in the high-latitude North Atlantic (Figure 3b) apparently remained lower than radiocarbon age offsets in both the contemporary Southern Ocean surface (Skinner et al., 2019), and the deep Iberi-

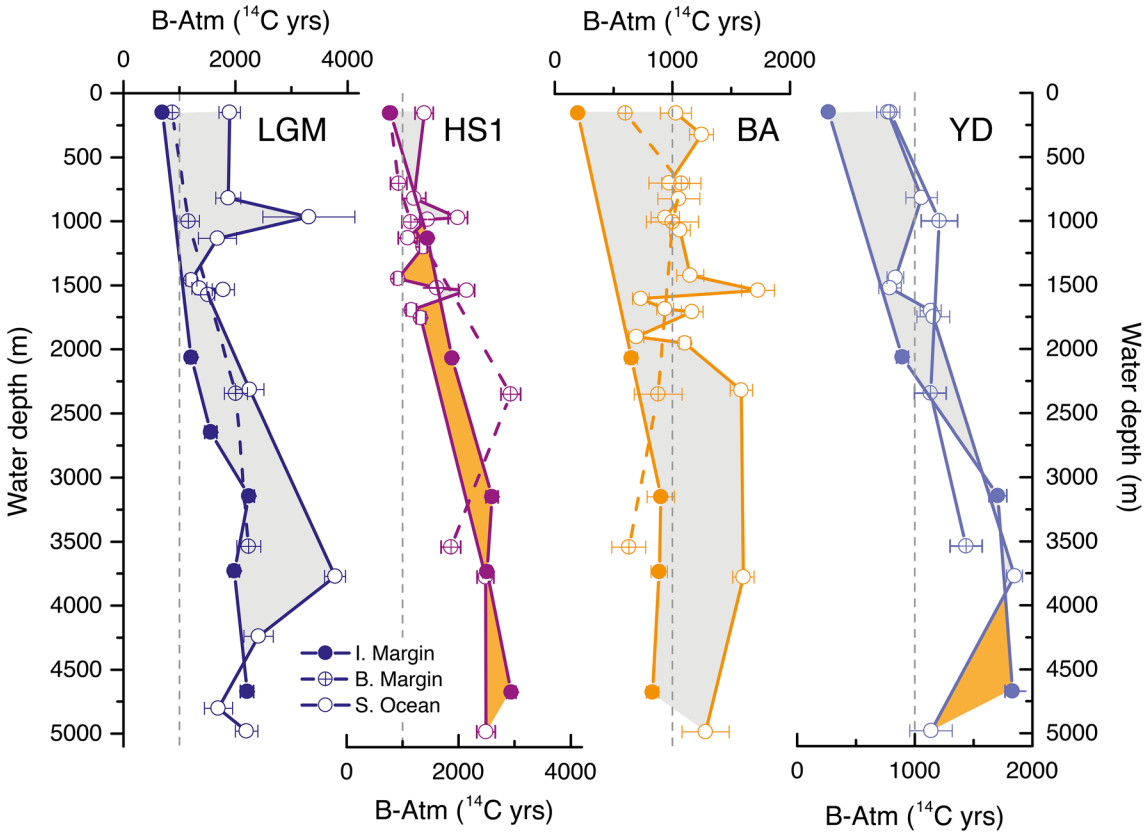

Figure 6. Depth profiles of ventilation age (B-Atm) for time-slices across the last deglaciation, from the Iberian Margin (filled symbols), Brazil Margin (crossed symbols), and Southern Ocean (open symbols; Zhao et al., 2018). The offset between the Iberian Margin (North Atlantic) and Southern Ocean is shaded (gray/orange indicates higher/lower B-Atm in the Southern Ocean), in order to illustrate periods where the radiocarbon ventilation gradient across the Atlantic collapsed or reversed, suggesting diminished supply of NADW to the Atlantic interior (i.e., during HS1, and to a lesser extent the YD). Despite overall reduced radiocarbon ventilation throughout the deep Atlantic, the ventilation gradient across the Atlantic at the LGM suggests active NADW export. HS1, Heinrich Stadial 1; LGM, Last Glacial Maximum; NADW, North Atlantic Deep Water; YD, Younger Dryas.

an Margin (Figure 3c), suggesting reduced export of NADW to the Iberian Margin, and possibly even a dominant source of ventilation from the Southern Ocean at this time (Menviel et al., 2018; Skinner et al., 2014).

Turning to paired $\delta^{13}C$ and radiocarbon profiles on the Brazil- and Iberian Margins (see Figure 7), we find two main differences between the vertical radiocarbon- and $\delta^{13}C$ gradients that help to shed light on the apparent decoupling of water-mass extent from water-mass ventilation states. The first difference (noted above) is that while radiocarbon and $\delta^{13}C$ both show a stepped weakening of vertical gradients between the LGM and the Holocene, the vertical gradient in $\delta^{13}C$ at the LGM was especially strong; far stronger than might be expected from the vertical radiocarbon gradient. This could imply that water bathing the deepest abyssal sites (most likely of southern origin, but possibly also with a northern contribution (Keigwin & Swift, 2017)), had a particularly high respired carbon content, and/or a particularly high (and positive) "biological disequilibrium carbon" content (Khatiwala et al., 2019). This situation would have contributed to atmospheric CO_2 draw-down at the LGM. Alternatively, and perhaps not exclusively, water bathing mid-depth sites (~2 km, and most likely of a predominantly northern origin) may have had a particularly low respired carbon content, and/or a particularly low (and negative) "physical disequilibrium carbon" content (Khatiwala et al., 2019). This situation would not, on its own, have contributed to atmospheric CO_2 draw-down at the LGM, since it would reflect an even stronger deficit of carbon uptake in the North Atlantic than exists today. The latter interpretation would be more consistent with the observation that it is the $\delta^{13}C$ at ~2 km water depth that seems anomalously positive at the LGM (Curry & Oppo, 2005), particularly for the radiocarbon ventilation at this water depth (Figure 7). The suggestion that glacial North Atlantic intermediate water (GNAIW) was less equilibrated with the atmosphere at the LGM, without acquiring a com-

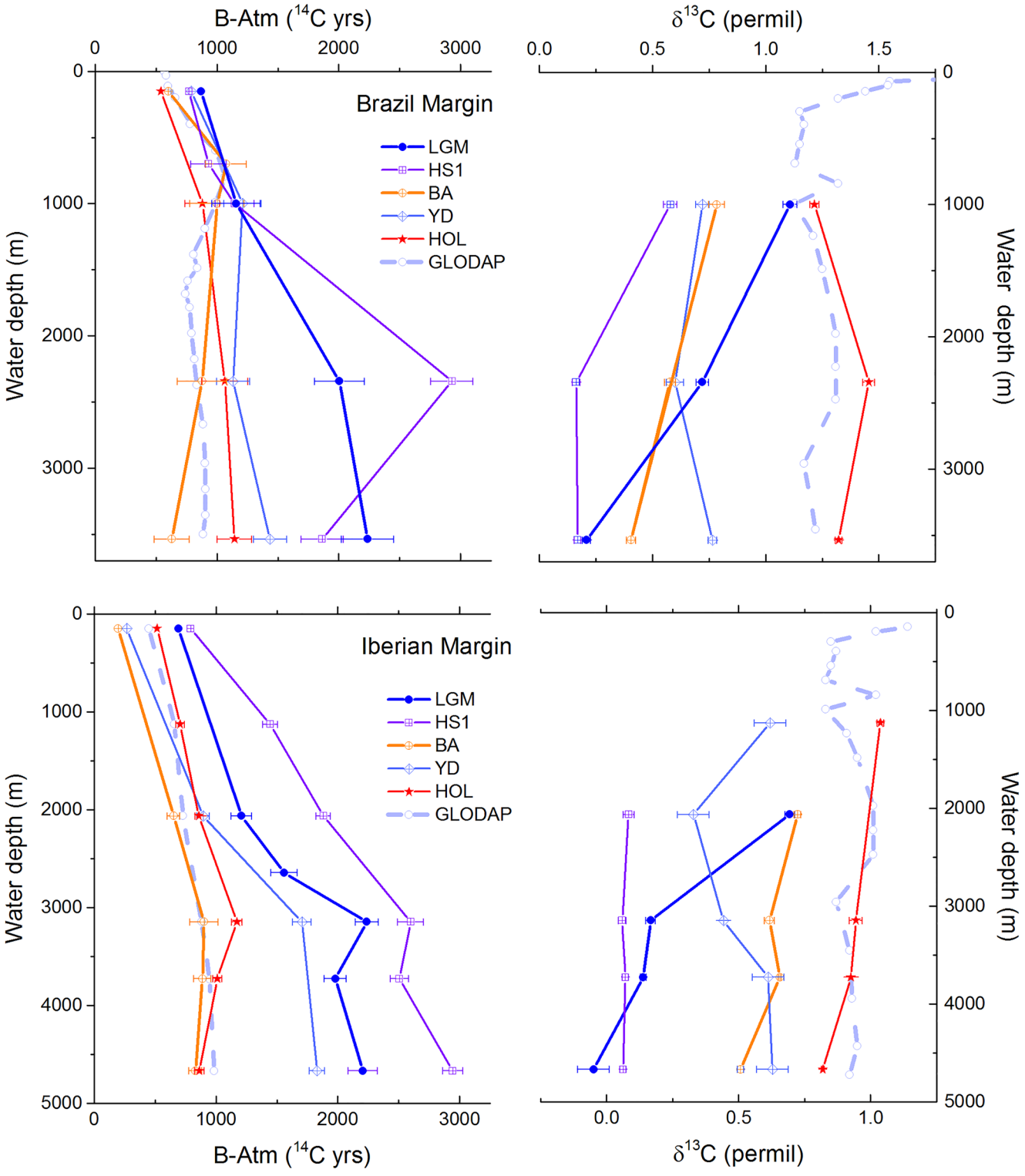

Figure 7. Depth profiles of ventilation age (B-Atm) (left) and δ^{13}C (right) on the Brazil Margin (upper) and Iberian Margin (lower). Surface reservoir-ages for each time-slice (consistent with the age-models for each sediment core) are used to provide values at an arbitrary depth of 250 m in each transect. The modern ventilation age is shown for each site (gray dashed lines with open circles; GLODAP, Key et al., 2004). Modern water column profiles of δ^{13}C measured on DIC are also shown for each margin (gray dashed lines with open circles; GEOSECS, Key et al., 2004).

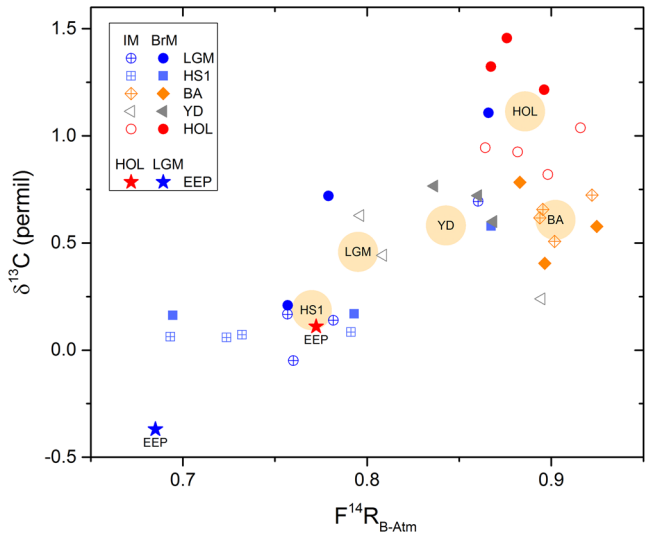

Figure 8. Cross plot of radiocarbon ventilation (expressed as a "relative enrichment" ratio, F14RB-Atm = exp (8033/B-Atm)) vs. epibenthic $\delta^{13}C$, for various time-slices across the last deglaciation. Each data point represents the time-slice average value in a given sediment core. Brazil Margin values are indicated by open symbols; Iberian Margin values are indicated by closed symbols. Different colors indicate the various time-slices: dark blue, LGM; light blue, HS1, orange, BA; gray, YD; red, HOL. Also shown for comparison are HOL and LGM values for the EEP (de la Fuente et al., 2015). Light orange circles indicate the average values for each time-slice, across both depth transects in the Atlantic; note how the BA appears to stand apart from the linear trend suggested by the HOL, YD, HS1, and LGM (as well as the EEP values), with relatively high radiocarbon activity for its $\delta^{13}C$. EEP, Eastern Equatorial Pacific; HOL, Holocene; HS1, Heinrich Stadial 1; LGM, Last Glacial Maximum; YD, Younger Dryas.

mensurate respired nutrient load, would appear to run contrary to the recent proposal that the carbon sequestration efficiency of GNAIW was enhanced at the LGM relative to that of NADW today (Yu et al., 2019). The latter proposal also sits uneasily with the observation of significantly larger radiocarbon reservoir age offsets in the high latitude North Atlantic at the LGM (e.g., Skinner et al., 2019; Thornalley et al., 2011), which indicate reduced air-sea CO_2 exchange efficiency as compared with today (in a region where CO_2 is generally taken up by the ocean (Takahashi et al., 2002)). A speculative reconciliation of these observations could be that CO_2 uptake in the North Atlantic was increased relative to today in absolute terms (due simply to enhanced solubility at lower temperature), even as the efficiency of CO_2 uptake was diminished (e.g., by sea ice, or shallow stratification). In this way, less CO_2 uptake would be achieved than would have been possible for constant air-sea exchange efficiency at LGM temperatures. This interpretation would resonate with a recent numerical model decomposition (Khatiwala et al., 2019), in which sea-ice and temperature contributions to marine CO_2 uptake act in opposition under LGM conditions. Although a quantitative reconciliation of the available radiocarbon, nutrient-, and carbonate ion reconstructions for the LGM North Atlantic remains to be achieved, the above discussion serves to emphasize that marine carbon uptake at the LGM most likely represented a nonlinear combination of partially opposing, and spatially variable, contributing factors.

The second main discrepancy between the radiocarbon- and $\delta^{13}C$ gradients shown in Figure 7 is that while the radiocarbon profiles on both the Iberian- and Brazil margins have reached a near-modern state by the B-A (with a subsequent small reversal at the YD), the $\delta^{13}C$ profiles remain offset from modern values by a significant amount (~−0.25 to −0.5 permil; see Figure 6). In part, this likely reflects the contribution of slow components of $\delta^{13}C$ change that were not directly linked to deglacial ocean circulation changes, for example, terrestrial biosphere expansion in particular (Yu et al., 2010), which would have caused marine $\delta^{13}C$ to rise between the BA and the late Holocene (Menviel & Joos, 2012). However, it is also notable that the range of $\delta^{13}C$ values expressed in the Atlantic water column, on the Brazil- and Iberian Margins, is not matched by a commensurate range in radiocarbon ventilation states. Low $\delta^{13}C$ values are also reported from the abyssal North Atlantic (>4.5 km) and in the deep South Atlantic (>3 km) during the BA ((Thiagarajan et al., 2014); and references within), despite radiocarbon ventilation ages suggesting an Atlantic Ocean dominated by well ventilated waters akin to NADW today.

The BA therefore appears to have represented a time of widespread air-sea equilibration and/or "flushing" of the Atlantic interior, where a range of different water masses of northern and southern origin (with different $\delta^{13}C$ signatures) continued to circulate in the Atlantic interior, albeit with particularly well-ventilated radiocarbon signatures. Once again, we note that these radiocarbon ventilation trends are not equivalent to mass transport trends indicated by Pa/Th. The end-member ventilation pulse during the BA is illustrated in Figure 8, where a broadly linear trend between $\delta^{13}C$ and radiocarbon ventilation (expressed as an isotopic ratio, or "relative enrichment" of the ocean vs. the contemporary atmosphere (Soulet et al., 2016)) is observed across the Atlantic, and into the deep Eastern Equatorial Pacific (EEP), for the LGM (Freeman, Skinner, Waelbroeck, et al., 2016), and all other time-slices since then, but not for the BA. The suggestion in Figure 8 is that the BA was a time of particularly strong ventilation (i.e., transport and/or air-sea equilibration) for all water masses filling the Atlantic basin. This would be consistent with the notion of an extreme deepening of the AMOC into the Southern Ocean during the BA (Barker et al., 2010), as well as the shift in the radiocarbon ventilation state of both northern and southern Atlantic deep-water end-members inferred from paired radiocarbon and Nd isotopes (Skinner et al., 2013). An Atlantic circulation that was similar, but

not identical, to the modern therefore appears to have been established at the BA, contributing to a particularly well-ventilated Atlantic at this time.

4.3. Carbon Cycle Implications: Ventilation Seesaws and Unresolved Puzzles

Our data serve to illustrate a succession of markedly different ocean circulation states in the Atlantic across the last deglaciation, specifically in terms of the evolving radiocarbon activity (and therefore the equilibration state of DIC in the ocean interior, relative to the atmosphere). Our LGM results echo previous findings, indicating reduced radiocarbon ventilation throughout the Atlantic (Skinner et al., 2017), an expanded volume of southern-sourced deep water, and consequently a strengthened vertical gradient in radiocarbon ventilation (Freeman, Skinner, Waelbroeck, et al., 2016), and especially in the $\delta^{13}C$ of DIC in the Atlantic (Curry et al., 1988). Our results also confirm the active export of northern sourced deep water at the LGM (Lippold et al., 2012; McManus et al., 2004; Ng et al., 2018), while emphasizing that this deep water was perhaps as poorly equilibrated with the atmosphere as modern southern sourced deep water, which in turn was in even greater disequilibrium (Skinner et al., 2019). While it seems clear that carbon isotope data from the Atlantic are consistent with an enhanced respired- and/or disequilibrium carbon inventory at the LGM (Khatiwala et al., 2019; Menviel et al., 2017; Muglia et al., 2018), there is no clear consensus on the relative dominance of the respired-versus disequilibrium-contributions. The relative contributions of slower turn-over rates (and organic carbon respiration rates) in the ocean interior, versus restricted air-sea gas exchange in regions where water retains a high positive (biological) disequilibrium DIC component, remain uncertain. Our data do not resolve this question, but they do emphasize a definite role for disequilibrium effects, and further help to illustrate why an expansion of southern-sourced deep water in the global ocean would have contributed to lower atmospheric CO_2 (Skinner, 2009), contrary to alternative proposals (Hain et al., 2011; Sigman et al., 2010). The reason for this is that southern sourced deep water, especially at the LGM (Sikes et al., 2000; Sikes et al., 2016; Skinner et al., 2010; Skinner et al., 2015; Skinner et al., 2017; Skinner et al., 2019), is characterized by poor equilibration with the atmosphere, and therefore a relatively high positive (biological) disequilibrium DIC concentration (Eggleston & Galbraith, 2018; Ito & Follows, 2013). The dominance of the deep ocean by a water mass with high positive disequilibrium DIC, at the expense of one with low (or negative) disequilibrium DIC, will tend to enhance the ocean's inventory of carbon that is sequestered from the atmosphere (Eggleston & Galbraith, 2018; Galbraith and Skinner, 2020; Khatiwala et al., 2019). Therefore, the fact that southern sourced deep water has a high concentration of "preformed nutrients" (i.e., respired nutrients that were advected to the surface ocean, and then advected back into the ocean interior without being fixed into organic matter) does not mean that a dominance of southern sourced water will diminish the efficiency of the biological pump, as long as those nutrients are associated with disequilibrium DIC (Eggleston & Galbraith, 2018; Galbraith and Skinner, 2020; Khatiwala et al., 2019). Here, we underline the radiocarbon depletion of the ocean interior at the LGM relative to the atmosphere (along with that of high latitude surface waters (Skinner et al., 2019)), as an indication that disequilibrium DIC levels were likely even more negative in northern sourced waters (mainly due to a "physical," or solubility related, deficit), and more positive in southern deep waters (mainly due to a "biological," respired carbon, excess). These changes would have had opposing impacts on atmospheric atmospheric CO_2 (Khatiwala et al., 2019), with the net effect on atmospheric CO_2 being controlled by the volume of the ocean that was influenced by southern sourced deep water (Eggleston & Galbraith, 2018; Galbraith and Skinner, 2020; Ito & Follows, 2013; Skinner, 2009). A change to the Atlantic chemistry alone (without significant "downstream" effects on the rest of the ocean) might be expected to have a minor impact on atmospheric CO_2 (Hain et al., 2014), due to the limited size of the Atlantic basin (~25% of the ocean volume (Menard & Smith, 1966)), and the limited volumetric significance of NADW (~21 % of the ocean volume (Johnson, 2008)).

The latter point may explain why the apparent quasi-elimination of radiocarbon delivery to the deep Atlantic via northern sourced deep-water during HS1 (which particularly affected water depths between ~1 and ~3 km in the Atlantic) was not associated with a further drop in atmospheric CO_2. On the contrary, atmospheric CO_2 increased across HS1 (whilst $\Delta^{14}C_{atm}$ and $\delta^{13}CO_{2\text{-}atm}$ decreased) (Bauska et al., 2016; Marcott et al., 2014; Monnin et al., 2001), most likely due to the limited impacts of carbon storage in a volumetrically restricted Atlantic basin (Hain et al., 2014), combined with the active release of radiocarbon-depleted CO_2

from other regions of the ocean, such as the Southern Ocean (Anderson et al., 2009; Burke & Robinson, 2012; Hines et al., 2015; Martinez-Boti et al., 2015; Skinner et al., 2010; Skinner et al., 2013; Skinner et al., 2014), or the Pacific Ocean (de la Fuente et al., 2015; Martinez-Boti et al., 2015; Rae et al., 2014). Notably, this does not preclude an important (or even a necessary) causal association between intermediate/mid-depth Atlantic circulation changes that may have contributed to enhanced (if limited) carbon storage (Lacerra et al., 2017; Schmittner & Lund, 2015), and other circulation/sea-ice changes that contributed directly to carbon release elsewhere in the global ocean, for example, via "ventilation seesaws" between the North Atlantic and North Pacific (Chikamoto et al., 2012; Freeman et al., 2015; Menviel et al., 2014; Okazaki et al., 2010) or between the North Atlantic and Southern Ocean (Anderson et al., 2009; Broecker, 1998; Menviel et al., 2015; Menviel et al., 2018; Skinner et al., 2014). The main impact of deglacial AMOC changes on atmospheric CO_2 may have therefore been via teleconnections to other regions of the world, and indirect effects on ocean-atmosphere exchanges in these regions.

A similar argument might be made for the BA, which was characterized by extremely well-ventilated conditions in the Atlantic, at least commensurate with modern, yet stable or slightly declining atmospheric CO_2, and relatively stable $\delta^{13}CO_{2\text{-atm}}$ (Bauska et al., 2016; Monnin et al., 2001). However, two things frustrate this argument, leading to an apparent puzzle regarding deglacial atmospheric CO_2 rise. The first difficulty is that, while the transition from the LGM to HS1 witnessed a relatively small change in the ventilation state that affected only a portion of the Atlantic interior (primarily between 1 and 3 km water depth), the transition from HS1 to the BA witnessed a very large change that appears to have affected the entire water column. A small direct effect on atmospheric CO_2 due to AMOC change in HS1 might be feasible, but the same would be harder to defend for the very large ventilation change experienced at the BA. The second difficulty is that, despite the apparent operation of a "bi-polar ventilation seesaw," characterized by alternating pulses of convection in the North Atlantic and Southern Ocean across Dansgaard-Oeschger (stadial-interstadial) variability (Broecker, 1998; Gottschalk et al., 2016; Jaccard et al., 2016; Menviel et al., 2015; Menviel et al., 2018; Skinner et al., 2014), the BA nevertheless seems to have been a period of increased ocean-atmosphere equilibration, relative to the LGM and HS1, for both northern and southern sourced deep-water (Skinner et al., 2013). This is further emphasized by the evidence for greater ocean-atmosphere equilibration in the deep southern, northern and equatorial Pacific during the BA, as compared to HS1 and/or the LGM (de la Fuente et al., 2015; Galbraith et al., 2007; Lindsay et al., 2016; Sikes et al., 2016; Skinner et al., 2015). A very large volume of the ocean was therefore better equilibrated with the atmosphere during the BA, as compared to the LGM or HS1. It seems plausible that most, if not all, of this volume of ocean would have possessed a pCO_2 higher than that of the atmosphere, prior to equilibration at the ocean surface, as indeed is suggested by surface ocean pH reconstructions from potential regions of deep convection, such as the Southern Ocean and North Pacific (Gray et al., 2018; Martinez-Boti et al., 2015). These reconstructions indicate elevated pCO_2 (relative to the atmosphere; hence active CO_2 release) during the BA (Gray et al., 2018; Martinez-Boti et al., 2015), which presents a puzzle: why did atmospheric CO_2 not rise (and $\delta^{13}CO_{2\text{-atm}}$ not decline) across the BA?

One approach to resolving this puzzle might be to note that atmospheric CO_2 would normally be expected to drop during a North Atlantic interstadial (Ahn & Brook, 2008; Bereiter et al., 2012; Wolff et al., 2009). There are a range of candidate contributors to the "natural" declining trend, including a cooling Southern Ocean (Marchal et al., 1998), an expanding terrestrial biosphere (Menviel et al., 2008), and/or renewed iron fertilization of Southern Ocean export productivity (Martinez-Garcia et al., 2014). Nevertheless, it is notable that the fate of atmospheric CO_2 during interstadials has received less direct attention than that of CO_2 during stadials (Gottschalk et al., 2019), making it hard to speculate on what occurred at these times with any degree of confidence. The efflux of carbon from the ocean to the atmosphere during the BA (expected on the basis of the radiocarbon and surface ocean pH evidence noted above), might therefore explain why CO_2 did not in fact drop, as has been suggested previously (Skinner et al., 2013). All of this would support the proposal that the BA was a "point of no return" in the deglacial process, precisely because of anomalously stable atmospheric CO_2 (Wolff et al., 2009).

Even if it can be shown that the especially strong ventilation of the Atlantic interior did help to keep atmospheric CO_2 relatively high across the BA (against other, as yet vaguely defined, processes), it would remain puzzling if the very large and abrupt "flushing" of the Atlantic that occurred at the onset of the BA did not

push up atmospheric CO_2 at all. Indeed, it seems plausible that this major ventilation change likely contributed to the centennial atmospheric CO_2 "jump" recorded at ~14.8 ka BP (Marcott et al., 2014). A similar case could be made for a second ventilation increase that appears to have accompanied the end of the YD. In this respect, our results confirming an increase in ventilation throughout the Atlantic interior at the onset of the BA (and rather less clearly at the end of the YD), would bolster the proposals of Chen et al. (2015) and Gray et al. (2018), for a direct AMOC role in centennial CO_2 jumps at these times. Nevertheless, available $\delta^{13}CO_{2\text{-atm}}$ evidence does not support an overwhelming oceanic source of carbon to the atmosphere at the onset of the BA (Bauska et al., 2016), and it is intriguing that atmospheric CO_2 jumped up by the same amount (~12–13 ppm) at both of these transitions (Marcott et al., 2014), whereas the increase in ventilation experienced in the Atlantic interior was clearly far greater at the onset of the BA than at the end of the YD. Furthermore, it remains unclear that any significant change in Atlantic ventilation (see Figure 5; also Chen et al., 2015), or distal upwelling (e.g., Rae et al., 2018), occurred in time with the third centennial CO_2 jump that is recorded at ~16.3 ka BP, during HS1 (Marcott et al., 2014). On the Iberian Margin, we find small increases in $\delta^{13}C$ (0.2–0.3‰) in 2 out of 4 records in the vicinity of 16.3 kyrs BP, when pCO_2 rises rapidly, however these are not well constrained, and a subtle increase in radiocarbon ventilation age is only observed at ~2.1 km water depth at this time. On the Brazil Margin, at 2.4 km depth, ventilation ages do decrease in the middle of HS1 (~15.8 kyrs) and $\delta^{13}C$ values are slightly higher, suggesting a short ventilation pulse may have influenced this site in the middle of HS1, though again this remains equivocal. Therefore, despite some tantalizing clues, higher resolution data are still needed to confirm whether or not rapid transient ventilation changes occurred ~16.3 ka. This arguably represents a key test of the proposition that past centennial scale changes in atmospheric CO_2 were consistently linked to Atlantic ventilation changes (Chen et al., 2015), as opposed to terrestrial carbon release, for example (Köhler et al., 2014), or indeed a mixture of drivers (Bauska et al., 2016).

5. Conclusions

Over the last deglaciation, the Atlantic Ocean circulation changed in association with abrupt climate events and changes in the atmospheric CO_2 level. These changes were associated with large shifts in the Atlantic Ocean's radiocarbon inventory, which at times led to very large offsets between oceanic and the atmospheric radiocarbon ages. Our reconstructions suggest that southern sourced deep water filled a greater volume of the Atlantic at the LGM, albeit with lesser impacts in the western basin, while NADW shoaled but remained active. During HS1, NADW was further reduced and shoaled relative to the LGM, but continued to influence the upper Atlantic Ocean. At the onset of the BA, the AMOC resumed and NADW expanded throughout the Atlantic interior, causing the entire basin to rapidly become at least as well ventilated as the modern Atlantic. However, parallel $\delta^{13}C$ measurements (as well as Nd isotopes (Skinner et al., 2013) and sedimentary Pa/Th (Gherardi et al., 2009)), suggest that the Atlantic circulation was nevertheless distinct from modern during the BA, with a greater influence of relatively well-ventilated southern sourced water. A short return to more poorly ventilated waters occurred during the YD, before the modern distribution of radiocarbon was obtained in the early Holocene.

These inferences broadly cohere with a familiar story of changing AMOC across the deglaciation, for example, as represented in its most general aspects by available Pa/Th reconstructions from the deep western Atlantic (McManus et al., 2004; Ng et al., 2018). However, some details merit special emphasis: first, the observational support for active northern sourced deep-water export at the LGM; second, a divide between the western- and eastern Atlantic, with the former affected less significantly by changes in the representation of northern and southern water masses, despite both being strongly affected by changes in the air-sea equilibration of both northern and southern deep water end-members; and finally, the occurrence of ventilation at least as strong as modern, resulting in a "flushing" of the entire Atlantic water column during the BA, both due to a reinvigoration of the AMOC (likely affecting depths <3 km primarily (Gherardi et al., 2009)), and due to an apparent increase in the air-sea equilibration of southern sourced deep water relative to the LGM and HS1.

Our findings bear on the mechanisms responsible for deglacial atmospheric CO_2 rise, which we suggest may be explained by a combination of: gradual carbon release during periods of reduced AMOC (i.e., HS1

and the YD), due to enhanced ventilation via the North Pacific and Southern Ocean at these times; and abrupt (albeit limited) carbon release as the AMOC resumed and flushed out the respired carbon inventory of the deep Atlantic (i.e., at the ends of HS1 and the YD). The relatively slow, millennial, release of carbon from outside the Atlantic Ocean during HS1 and the YD might therefore be related to the larger volume and longer response time of the deep Southern Ocean and Indo-Pacific carbon pools, whereas the more abrupt and transient centennial carbon release from the Atlantic Ocean would reflect the smaller respired carbon inventory and rapid response time of this basin (Hain et al., 2014). However, the rapid increase in atmospheric CO_2 in the middle of HS1, around 16.3 kyrs BP, only tentatively fits into this framework, as we find (at best) ambiguous evidence for any change in the Atlantic Ocean ventilation/circulation at this time, consistent with previous work (Chen et al., 2015; Rae et al., 2018). Whilst it is possible that the cause of the atmospheric CO_2 increase at 16.3 kyrs BP was distinct from those at 14.8 and 11.7 kyrs BP, tentative anomalies in our data from the Iberian and Brazil Margins, as well as some radiocarbon evidence from the high latitude North Atlantic (Thornalley et al., 2011; Thornalley et al., 2015), suggest that the occurrence of centennial-scale variability in Atlantic radiocarbon ventilation across HS1 should not be ruled out just yet. A larger number of higher resolution ventilation records of HS1 will be needed to resolve this puzzle. A further puzzle emerges concerning the relative stability of atmospheric CO_2 across the B-A, despite clear evidence for strong ventilation of the ocean interior, at least commensurate with the modern ocean, throughout the Atlantic, and likely much of the rest of the global ocean. We suggest that a solution to this puzzle might derive from a better understanding of the processes that act to draw down atmospheric CO_2 during "normal" interstadial conditions, outside of deglaciations. By counteracting these processes, an especially strong shift in ocean ventilation at the BA (Barker et al., 2010), could have stabilized atmospheric $CO_2$2 and thus brought about a critical turning point in the deglacial process (Wolff et al., 2009).

Data Availability Statement

Datasets for this research are included in this paper (and its supporting information files), and are also available at: https://doi.pangaea.de/10.1594/PANGAEA.925638

Acknowledgments
We would like to thank James Rolfe and Ian Mather for stable isotope measurements, Simon Crowhurst for XRF core scanning, Ron Reimer for performing the AMS measurements at the 14CHRONO Centre in Belfast, and Trond Dokken for provision of sample material and XRF data from Brazil Margin cores. L. C. Skinner acknowledges support for this work from the Natural Environment Research Council, though cruise JC089 (NE/J00653X/1) and NERC grant NE/L006421/1, as well as support from the Royal Society and the Isaac Newton Trust. MD09 cores were collected by the R/V Marion Dufresne during RETRO Cruise II, supported by ESF EUROMARC project RETRO, IPEV, and ANR project ANR-09-BLAN-0347. C. Waelbroeck acknowledges support from the European Research Council grant ACCLIMATE/no 339108. We are also grateful for the helpful comments of two anonymous reviewers, and the associate editor, on an earlier draft of this manuscript.

References

Adkins, J. F. (2013). The role of deep ocean circulation in setting glacial climates. *Paleoceanography*, *28*, 539–561.
Ahn, J., & Brook, E. J. (2008). Atmospheric CO_2 and climate on millennial time scales during the last glacial period. *Science*, *322*, 83–85.
Anderson, R. F., Ali, S., Bradtmiller, L. I., Nielsen, S. H. H., Fleisher, M. Q., Anderson, B. E., & Burckle, L. H. (2009). Wind-driven upwelling in the Southern Ocean and the deglacial rise in atmospheric CO_2. *Science*, *323*, 1443–1448.
Barker, S., Diz, P., Vautravers, M., Pike, J., Knorr, G., Hall, I. R., & Broecker, W. (2009). Interhemispheric Atlantic seesaw response during the last deglaciation. *Nature*, *457*, 1097–1102.
Barker, S., Knorr, G., Vautravers, M., Diz, P., & Skinner, L. C. (2010). Extreme deepening of the Atlantic overturning circulation during deglaciation. *Nature Geoscience*, *3*, 567–571. https://doi.org/10.1038/NGEO921
Bauska, T. K., Baggenstos, D., Brook, E. J., Mix, A. C., Marcott, S. A., Petrenko, V. V., et al. (2016). Carbon isotopes characterize rapid changes in atmospheric carbon dioxide during the last deglaciation. *Proceedings of the National Academy of Sciences*, *113*, 3465–3470.
Bereiter, B., Lüthi, D., Siegrist, M., Schüpbach, S., Stocker, T. F., & Fischer, H. (2012). Mode change of millennial CO_2 variability during the last glacial cycle associated with a bipolar marine carbon seesaw. *Proceedings of the National Academy of Sciences*, *109*, 9755–9760.
Björck, S., Walker, M. J. C., Cwynar, L. C., Johnsen, S., Knudsen, K.-L., Lowe, J. J., & Wohlfarth, B., & INTIMATE Group (1998). An event stratigraphy for the last termination in the North Atlantic region based on the Greenland ice-core record: A proposal by the INTIMATE group. *Journal of Quaternary Science*, *13*, 283–292.
Blunier, T., & Brook, E. J. (2001). Timing of millennial-scale climate change in Antarctica and Greenland during the last glacial period. *Science*, *291*, 109–112.
Böhm, E., Lippold, J., Gutjahr, M., Frank, M., Blaser, P., Antz, B., et al. (2014). Strong and deep Atlantic meridional overturning circulation during the last glacial cycle. *Nature*, *517*, 73–76.
Bradtmiller, L. I., McManus, J. F., & Robinson, L. F. (2014). 231Pa/230Th evidence for a weakened but persistent Atlantic meridional overturning circulation during Heinrich Stadial 1. *Nature Communications*, *5*, 5817.
Broecker, W. S. (1998). Palaeocean circulation during the last deglaciation: A bipolar seesaw? *Paleoceanography*, *13*, 119–121.
Burckel, P., Waelbroeck, C., Gherardi, J. M., Pichat, S., Arz, H., Lippold, J., et al. (2015). Atlantic Ocean circulation changes preceded millennial tropical South America rainfall events during the last glacial. *Geophysical Research Letters*, *42*(2), 411–418. https://doi.org/10.1002/2014GL062512
Burke, A., & Robinson, L. F. (2012). The Southern Ocean's role in carbon exchange during the last deglaciation. *Science*, *335*, 557–561.
Butzin, M., Köhler, P., & Lohmann, G. (2017). Marine radiocarbon reservoir age simulations for the past 50,000 years. *Geophysical Research Letters*, *44*(16), 8473–8480. https://doi.org/10.1002/2017GL074688
Came, R. E., Oppo, D. W., & Curry, W. B. (2003). Atlantic Ocean circulation during the Younger Dryas: Insights from a new Cd/Ca record from the western subtropical South Atlantic. *Paleoceanography*, *18*, 1086. https://doi.org/10.1029/2003PA000888
Cheng, H., Edwards, R. L., Broecker, W. S., Denton, G. H., Kong, X. G., Wang, Y. J., et al. (2009). Ice age terminations. *Science*, *326*, 248–252.

Cheng, H., Sinha, A., Cruz, F. W., Wang, X., Edwards, R. L., d'Horta, F. M., et al. (2013). Climate change patterns in Amazonia and biodiversity. *Nature Communications*, *4*, 1411.

Chen, T., Robinson, L. F., Burke, A., Southon, J., Spooner, P., Morris, P. J., & Ng, H. C. (2015). Synchronous centennial abrupt events in the ocean and atmosphere during the last deglaciation. *Science*, *349*, 1537–1541.

Chikamoto, M. O., Menviel, L., Abe-Ouchi, A., Ohgaito, R., Timmermann, A., Okazaki, Y., et al. (2012). Variability in North Pacific intermediate and deep water ventilation during Heinrich events in two coupled climate models. *Deep Sea Research Part II: Topical Studies in Oceanography*, *61–64*, 114–126.

Clark, P. U., Pisias, N. G., Stocker, T. F., & Weavers, A. J. (2002). The role of the thermohaline circulation in abrupt climate change. *Nature*, *415*, 863–869.

Curry, W. B., Duplessy, J. C., Labeyrie, L. D., & Shackleton, N. J. (1988). Changes in the distribution of d13C of deep water sigma-CO_2 between the last glaciation and the Holocene. *Paleoceanography*, *3*, 317–341.

Curry, W. B., & Lohmann, G. (1983). Reduced advection into Atlantic Ocean deep eastern basins during last glaciation maximum. *Nature*, *306*, 577–580.

Curry, W. B., & Oppo, D. W. (2005). Glacial water mass geometry and the distribution of d13C of Sigma-CO_2 in the western Atlantic Ocean. *Paleoceanography*, *20*, PA1017.

de Abreu, L. (2000). *High resolution Paleoceanography off Portugal during the last two glacial cycles.* Department of Earth Sciences. Cambridge: University of Cambridge.

de la Fuente, M., Skinner, L., Calvo, E., Pelejero, C., & Cacho, I. (2015). Increased reservoir ages and poorly ventilated deep waters inferred in the glacial Eastern Equatorial Pacific. *Nature Communications*, *6*, 7420. https://doi.org/10.1038/ncomms8420

Denton, G. H., Anderson, R. F., Toggweiler, J. R., Edwards, R. L., Schaefer, J. M., & Putnam, A. E. (2010). The last glacial termination. *Science*, *328*, 1652–1656.

Diz, P., & Barker, S. (2015). Linkages between rapid climate variability and deep-sea benthic foraminifera in the deep Subantarctic South Atlantic during the last 95 kyr. *Paleoceanography*, *30*, 601–611.

Dokken, T. M., Nisancioglu, K. H., Li, C., Battisti, D. S., & Kissel, C. (2013). Dansgaard-Oeschger cycles: Interactions between ocean and sea ice intrinsic to the Nordic seas. *Paleoceanography*, *28*, 491–502.

Eggleston, S., & Galbraith, E. D. (2018). The devil's in the disequilibrium: Multi-component analysis of dissolved carbon and oxygen changes under a broad range of forcings in a general circulation model. *Biogeosciences*, *15*(12), 3761–3777. https://doi.org/10.5194/bg-15-3761-2018

Freeman, E., Skinner, L., Reimer, R., Scrivner, A., & Fallon, S. (2016). Graphitization of small carbonate samples for paleoceanographic Research at the Godwin Radiocarbon Laboratory, University of Cambridge. *Radiocarbon*, *58*(1), 89–97. https://doi.org/10.1017/RDC.2015.8

Freeman, E., Skinner, L. C., Tisserand, A., Dokken, T., Timmermann, A., Menviel, L., & Friedrich, T. (2015). An Atlantic-Pacific ventilation seesaw across the last deglaciation. *Earth and Planetary Science Letters*, *424*, 237–244.

Freeman, E., Skinner, L., Waelbroeck, C., & Hodell, D. (2016). Radiocarbon evidence for enhanced respired carbon storage in the deep Atlantic at the Last Glacial Maximum. *Nature Communications*, *7*.

Galbraith, E., Jaccard, S. L., Pedersen, T. F., Sigman, D. M., Haug, G. H., Cook, M., et al. (2007). Carbon dioxide release from the North Pacific abyss during the last deglaciation. *Nature*, *449*, 890–893.

Galbraith, E., Kwon, E. Y., Bianchi, D., Hain, M. P., & Sarmiento, J. L. (2015). The impact of atmospheric pCO_2 on carbon isotope ratios of the atmosphere and ocean. *Global Biogeochemical Cycles*, *29*, 307–324. https://doi.org/10.1002/2014GB004929

Galbraith, E. D., & Skinner, L. C. (2020). The biological pump during the last glacial maximum. *Annual Review of Marine Science*, *12*, 559–586.

Ganopolski, A., & Rahmstorf, S. (2001). Rapid changes of glacial climate simulated in a coupled climate model. *Nature*, *409*, 153–158.

Gherardi, J.-M., Labeyrie, L., McManus, J. F., Francois, R., Skinner, L. C., & Cortijo, E. (2005). Evidence from the North Eastern Atlantic basin for variability of the meridional overturning circulation through the last deglaciation. *Earth and Planetary Science Letters*, *240*, 710–723.

Gherardi, J.-M., Labeyrie, L., Nave, S., Francois, R., McManus, J. F., & Cortijo, E. (2009). Glacial-interglacial circulation changes inferred from 231Pa/230Th sedimentary record in the North Atlantic region. *Paleoceanography*, *24*. PA2204. https://doi.org/10.1029/2008PA001696

Gottschalk, J., Battaglia, G., Fischer, H., Frölicher, T. L., Jaccard, S. L., Jeltsch-Thömmes, A., et al. (2019). Mechanisms of millennial-scale atmospheric CO_2 change in numerical model simulations. *Quaternary Science Reviews*, *220*, 30–74.

Gottschalk, J., Skinner, L. C., Lippold, J., Vogel, H., Frank, N., Jaccard, S. L., & Waelbroeck, C. (2016). Biological and physical controls in the Southern Ocean on past millennial-scale atmospheric CO_2 changes. *Nature Communications*, *7*, 11539.

Gray, W. R., Rae, J. W. B., Wills, R. C. J., Shevenell, A. E., Taylor, B., Burke, A., et al. (2018). Deglacial upwelling, productivity and CO_2 outgassing in the North Pacific Ocean. *Nature Geoscience*, *11*(5), 340–344. https://doi.org/10.1038/s41561-018-0108-6

Hain, M. P., Sigman, D. M., & Haug, G. H. (2011). Shortcomings of the isolated abyssal reservoir model for deglacial radiocarbon changes in the mid-depth Indo-Pacific Ocean. *Geophysical Research Letters*, *38*(4), L0460410. https://doi.org/10.1029/2010gl046158

Hain, M. P., Sigman, D. M., & Haug, G. H. (2014). Distinct roles of the Southern Ocean and North Atlantic in the deglacial atmospheric radiocarbon decline. *Earth and Planetary Science Letters*, *394*, 198–208.

Hines, S. K. V., Southon, J. R., & Adkins, J. F. (2015). A high-resolution record of Southern Ocean intermediate water radiocarbon over the past 30,000 years. *Earth and Planetary Science Letters*, *432*, 46–58.

Ito, T., & Follows, M. (2013). Air-sea disequilibrium of carbon dioxide enhances the biological carbon sequestration in the Southern Ocean. *Global Biogeochemical Cycles*, *27*, 1129–1138. https://doi.org/10.1002/2013GB004682

Jaccard, S. L., Galbraith, E. D., Martínez-García, A., & Anderson, R. F. (2016). Covariation of deep Southern Ocean oxygenation and atmospheric CO_2 through the last ice age. *Nature*, *530*, 207–210.

Johnson, G. C. (2008). Quantifying Antarctic Bottom water and North Atlantic deep water volumes. *Journal of Geophysical Research*, *113*, C05027. https://doi.org/10.1029/2007JC004477

Jonkers, L., Zahn, R., Thomas, A., Henderson, G., Abouchami, W., François, R., et al. (2015). Deep circulation changes in the central South Atlantic during the past 145 kyrs reflected in a combined 231Pa/230Th, Neodymium isotope and benthic record. *Earth and Planetary Science Letters*, *419*, 14–21.

Keigwin, L. D., & Lehmann, S. J. (1994). Deep circulation change linked to Heinrich event 1 and Younger Dryas in a mid-depth North Atlantic core. *Paleoceanography*, *9*, 185–194.

Keigwin, L. D., & Schlegel, M. A. (2002). Ocean ventilation and sedimentation since the glacial maximum at 3 km in the western North Atlantic. *Geochemistry, Geophysics, Geosystems*, *3*(6), 1–14. https://doi.org/10.1029/2001gc000283

Keigwin, L. D., & Swift, S. A. (2017). Carbon isotope evidence for a northern source of deep water in the glacial western North Atlantic. *Proceedings of the National Academy of Sciences.114*(11), 2831–2835. https://doi.org/10.1073/pnas.1614693114

Key, R. M., Kozyr, A., Sabine, C., Lee, K., Wanninkhof, R., Bullister, J. L., et al. (2004). A global ocean carbon climatology: Results from the global data analysis project (GLODAP). *Global Biogeochemical Cycles*, *18*(4), 1–23. https://doi.org/10.1029/2004GB002247

Khatiwala, S., Muglia, J., & Schmittner, A. (2019). Air-sea disequilibrium enhances ocean carbon storage during glacila periods. *Science Advances*, *5*, 1–10.

Kohler, P., Joos, F., Gerber, S., & Knutti, R. (2005). Simulated changes in vegetation distribution, land carbon storage, and atmospheric CO2 in response to a collapse of the North Atlantic thermohaline circulation. *Climate Dynamics*, *25*(7), 689–708. https://doi.org/10.1007/s00382-005-0058-8

Köhler, P., Knorr, G., & Bard, E. (2014). Permafrost thawing as a possible source of abrupt carbon release at the onset of the Bølling/Allerød. *Nature Communications*, *5*, 5520.

Lacerra, M., Lund, D., Yu, J., & Schmittner, A. (2017). Carbon storage in the mid-depth Atlantic during millennial-scale climate events. *Paleoceanography*, *32*, 780–795.

Lindsay, C. M., Lehman, S. J., Marchitto, T. M., Carriquiry, J. D., & Ortiz, J. D. (2016). New constraints on deglacial marine radiocarbon anomalies from a depth transect near Baja California. *Paleoceanography*, *31*, 1103–1116.

Lippold, J., Luo, Y., Francois, R., Allen, S. E., Gherardi, J., Pichat, S., et al. (2012). Strength and geometry of the glacial Atlantic meridional overturning circulation. *Nature Geoscience*, *5*, 813–816. https://doi.org/10.1038/ngeo1608

Lund, D. C., Tessin, A. C., Hoffman, J. L., & Schmittner, A. (2015). Southwest Atlantic water mass evolution during the last deglaciation. *Paleoceanography*, *30*, 477–494.

Lynch-Steiglitz, J., Stocker, T. F., Broecker, W., & Fairbanks, R. G. (1995). The influence of air-sea exchange on the isotopic composition of oceanic carbon: Observations and modeling. *Global Biogeochemical Cycles*, *9*, 653–665.

Marchal, O., Stocker, T. F., & Joos, F. (1998). Impact of oceanic reorganisations on the ocean carbon cycle and atmospheric carbon dioxide content. *Paleoceanography*, *13*, 225–244.

Marcott, S. A., Bauska, T. K., Buizert, C., Steig, E. J., Rosen, J. L., Cuffey, K. M., et al. (2014) Centennial-scale changes in the global carbon cycle during the last deglaciation. *Nature 514*, 616.

Martinez-Boti, M. A., Marino, G., Foster, G. L., Ziveri, P., Henehan, M. J., Rae, J. W. B., et al. (2015). Boron isotope evidence for oceanic carbon dioxide leakage during the last deglaciation. *Nature*, *518*, 219–222.

Martinez-Garcia, A., Sigman, D. M., Ren, H. J., Anderson, R. F., Straub, M., Hodell, D. A., et al. (2014). Iron fertilization of the subantarctic Ocean during the last ice age. *Science*, *343*, 1347–1350.

Martrat, B., Grimalt, J. O., Shackleton, N. J., de Abreu, L., Hutterli, M. A., & Stocker, T. F. (2007). Four climatic cycles of recurring deep and surface water destabilizations on the Iberian Margin. *Science*, *317*, 502–507.

McManus, J. F., Francois, R., Gherardi, J.-M., Keigwin, L. D., & Brown-Leger, S. (2004). Collapse and rapid resumption of the Atlantic meridional circulation linked to deglacial climate changes. *Nature*, *428*, 834–837.

Menard, H. W., & Smith, S. M. (1966). Hypsometry of ocean basin provinces. *Journal of Geophysical Research*, *71*, 4305–4325.

Menviel, L., England, M. H., Meissner, K. J., Mouchet, A., & Yu, J. (2014). Atlantic-Pacific seesaw and its role in outgassing CO_2 during Heinrich events. *Paleoceanography*, *29*, 58–70.

Menviel, L., & Joos, F. (2012). Toward explaining the Holocene carbon dioxide and carbon isotope records: Results from transient ocean carbon cycle-climate simulations. *Paleoceanography*, *27*.

Menviel, L., Spence, P., & England, M. H. (2015). Contribution of enhanced Antarctic Bottom Water formation to Antarctic warm events and millennial-scale atmospheric CO_2 increase. *Earth and Planetary Science Letters*, *413*, 37–50.

Menviel, L., Spence, P., Yu, J., Chamberlain, M. A., Matear, R. J., Meissner, K. J., & England, M. H. (2018). Southern Hemisphere westerlies as a driver of the early deglacial atmospheric CO_2 rise. *Nature Communications*, *9*, 2503.

Menviel, L., Timmermann, A., Mouchet, A., & Timm, O. (2008). Meridional reorganizations of marine and terrestrial productivity during Heinrich events. *Paleoceanography*, *23*. PA1203. https://doi.org/10.1029/2007PA001445

Menviel, L., Yu, J., Joos, F., Mouchet, A., Meissner, K. J., & England, M. H. (2017). Poorly ventilated deep ocean at the last glacial maximum inferred from carbon isotopes: A data-model comparison study. *Paleoceanography*, *32*, 2–17.

Missiaen, L., Waelbroeck, C., Pichat, S., Jaccard, S. L., Eynaud, F., Greenop, R., & Burke, A. (2019). Improving North Atlantic marine core chronologies using 230Th normalization. *Paleoceanography and Paleoclimatology*, *34*, 1057–1073.

Monnin, E., Indermuhle, A., Dallenbach, A., Fluckiger, J., Stauffer, B., Stocker, T. F., et al. (2001). Atmospheric CO_2 concentrations over the last glacial termination. *Science*, *291*, 112–114.

Muglia, J., Skinner, L. C., & Schmittner, A. (2018). Weak overturning circulation and high Southern Ocean nutrient utilization maximized glacial ocean carbon. *Earth and Planetary Science Letters*, *496*, 47–56.

Muscheler, R., Beer, J., Wagner, G., Laj, C., Kissel, C., Raisbeck, G. M., et al. (2004). Changes in the carbon cycle during the last deglaciation as indicated by the comparison of ^{10}Be and ^{14}C records. *Earth and Planetary Science Letters*, *219*, 325–340.

Ng, H. C., Robinson, L. F., McManus, J. F., Mohamed, K. J., Jacobel, A. W., Ivanovic, R. F., et al. (2018). Coherent deglacial changes in western Atlantic Ocean circulation. *Nature Communications*, *9*, 2947.

Okazaki, Y., Timmermann, A., Menviel, L., Harada, N., Abe-Ouchi, A., Chikamoto, M. O., et al. (2010). Deepwater formation in the North Pacific during the last glacial termination. *Science*, *329*, 200–204.

Oppo, D. W., & Lehman, S. J. (1993). Mid-depth circulation of the subpolar North Atlantic during the last glacial maximum. *Science*, *259*, 1148–1152.

Parnell, A. C., Haslett, J., Allen, J. R. M., Buck, C. E., & Huntley, B. (2008). A flexible approach to assessing synchroneity of past events using Bayesian reconstructions of sedimentation history. *Quaternary Science Reviews*, *27*, 1872–1855.

Piotrowski, A. M., Galy, A., Nicholl, J. A. L., Roberts, N., Wilson, D. J., Clegg, J. A., & Yu, J. (2012). Reconstructing deglacial North and South Atlantic deep water sourcing using foraminiferal Nd isotopes. *Earth and Planetary Science Letters*, *357*, 289–297.

Piotrowski, A. M., Goldstein, S. L., Hemming, S. R., & Fairbanks, R. G. (2004). Intensification and variability of ocean thermohaline circulation through the last deglaciation. *Earth and Planetary Science Letters*, *225*, 205–220.

Pöppelmeier, F., Gutjahr, M., Blaser, P., Keigwin, L. D., & Lippold, J. (2018). Origin of abyssal NW Atlantic water masses since the last glacial maximum. *Paleoceanography and Paleoclimatology*, *33*, 530–543.

Rae, J. W. B., Burke, A., Robinson, L. F., Adkins, J. F., Chen, T., Cole, C., et al. (2018). CO_2 storage and release in the deep Southern Ocean on millennial to centennial timescales. *Nature*, *562*, 569–573.

Rae, J. W. B., Sarnthein, M., Foster, G. L., Ridgwell, A., Grootes, P. M., & Elliott, T. (2014). Deep water formation in the North Pacific and deglacial CO_2 rise. *Paleoceanography*, *29*, 645–667.

Reimer, P. J., Bard, E., Bayliss, A., Beck, J. W., Blackwell, P. G., Ramsey, C. B., et al. (2013). INTCAL13 and MARINE13 radiocarbon age calibration curves 0-50,000 years cal BP. *Radiocarbon*, *55*, 1869–1887.

Roberts, N. L., Piotrowski, A. M., McManus, J. F., & Keigwin, L. D. (2010). Synchronous deglacial overturning and water mass source changes. *Science*, *327*, 75–78.

Robinson, L. F., Adkins, J. F., Keigwin, L. D., Southon, J., Fernandez, D. P., Wang, S.-L., & Scheirer, D. S. (2005). Radiocarbon variability in the western North Atlantic during the last deglaciation. *Science*, *310*, 1469–1473.

Ruth, U., Wagenbach, D., Steffensen, J. P., & Bigler, M. (2003). Continuous record of microparticle concentration and size distribution in the central Greenland NGRIP ice core during the last glacial period. *Journal of Geophysical Research: Atmosphere*, *108*(D3), 4098. https://doi.org/10.1029/2002JD002376

Sarnthein, M., Winn, K., Jung, S. J. A., Duplessy, J.-C., Erlenkauser, H., Flatoy, A., et al. (1994). Changes in east Atlantic deep-water circulation over the last 30,000 years: Eight time-slice reconstructions. *Paleoceanography*, *9*, 209–267.

Schmittner, A., & Lund, D. C. (2015). Early deglacial Atlantic overturning decline and its role in atmospheric CO_2 rise inferred from carbon isotopes ($\delta^{13}C$). *Climate of the Past*, *11*, 135–152.

Schmittner, A., Saenko, O. A., & Weaver, A. J. (2003). Coupling of the hemispheres in observations and simulations of glacial climate change. *Quaternary Science Reviews*, *22*, 659–671.

Seidov, D., & Maslin, M. (2001). Atlantic Ocean heat piracy and the bipolar climate see-saw during Heinrich and Dansgaard-Oeschger events. *Journal of Quaternary Science*, *16*, 321–328.

Sigman, D. M., Hain, M. P., & Haug, G. H. (2010). The polar ocean and glacial cycles in atmospheric CO_2. *Nature*, *466*, 47–55.

Sikes, E. L., Cook, M. S., & Guilderson, T. P. (2016). Reduced deep ocean ventilation in the Southern Pacific Ocean during the last glaciation persisted into the deglaciation. *Earth and Planetary Science Letters*, *438*, 130–138.

Sikes, E. L., Samson, C. R., Guilderson, T. P., & Howard, W. R. (2000). Old radiocarbon ages in the southwest Pacific Ocean during the last glacial period and deglaciation. *Nature*, *405*, 555–559.

Skinner, L. C. (2009). Glacial-interglacial atmospheric CO_2 change: A possible standing volume effect on deep ocean carbon sequestration. *Climate of the Past*, *5*, 537–550.

Skinner, L. C., Fallon, S., Waelbroeck, C., Michel, E., & Barker, S. (2010). Ventilation of the deep Southern Ocean and deglacial CO_2 rise. *Science*, *328*, 1147–1151.

Skinner, L., McCave, I. N., Carter, L., Fallon, S., Scrivner, A., & Primeau, F. (2015). Reduced ventilation and enhanced magnitude of the deep Pacific carbon pool during the last glacial period. *Earth and Planetary Science Letters*, *411*, 45–52.

Skinner, L. C., Muschitiello, F., & Scrivner, A. E. (2019). Marine reservoir age variability over the last deglaciation: Implications for marine CarbonCycling and prospects for regional radiocarbon calibrations. *Paleoceanography and Paleoclimatology*, *34*, 1807–1815.

Skinner, L. C., Primeau, F., Freeman, E., de la Fuente, M., Goodwin, P., Gottschalk, J., et al. (2017). Radiocarbon constraints on the 'glacial' ocean circulation and its impact on atmospheric CO_2. *Nature Communications*, *8*, 16010.

Skinner, L. C., Scrivner, A., Vance, D., Barker, S., Fallon, S., & Waelbroeck, C. (2013). North Atlantic versus Southern Ocean contributions to a deglacial surge in deep ocean ventilation. *Geology*, *41*, 667–670. https://doi.org/10.1130/G34133.1

Skinner, L. C., & Shackleton, N. J. (2004). Rapid transient changes in Northeast Atlantic deep-water ventilation-age across Termination I. *Paleoceanography*, *19*, 1–11.

Skinner, L. C., & Shackleton, N. J. (2006). Deconstructing terminations I and II: Revisiting the glacioeustatic paradigm based on deep-water temperature estimates. *Quaternary Science Reviews*, *25*, 3312–3321.

Skinner, L. C., Shackleton, N. J., & Elderfield, H. (2003). Millennial-scale variability of deep-water temperature and d18Odw indicating deep-water source variations in the Northeast Atlantic, 0-34 cal. ka BP. *Geochemistry, Geophysics, Geosystems*, *4*(12), 1–17. https://doi.org/10.1029/2003GC000585

Skinner, L. C., Waelbroeck, C., Scrivner, A., & Fallon, S. (2014). Radiocarbon evidence for alternating northern and southern sources of ventilation of the deep Atlantic carbon pool during the last deglaciation. *Proceedings of the National Academy of Sciences*, *111*, 5480–5484.

Soulet, G. (2015). Methods and codes for reservoir-atmosphere ^{14}C age offset calculations. *Quaternary Geochronology*, *29*, 97–103. https://doi.org/10.1016/j.quageo.2015.05.023

Soulet, G., Skinner, L., Beaupre, S. R., & Galy, V. (2016). A note on reporting of reservoir ^{14}C disequilibria and age offsets. *Radiocarbon*, *57*.

Southon, J., Noronha, A. L., Cheng, H., Edwards, R. L., & Wang, Y. (2012). A high-resolution record of atmospheric C-14 based on Hulu Cave speleothem H82. *Quaternary Science Reviews*, *33*, 32–41.

Stern, J. V., & Lisiecki, L. E. (2013). North Atlantic circulation and reservoir age changes over the past 41,000years. *Geophysical Research Letters*, *40*(14), 3693–3697. https://doi.org/10.1002/grl.50679

Stuiver, M., & Polach, H. A. (1977). Reporting of ^{14}C data. *Radiocarbon*, *19*, 355–363.

Svensson, A., Andersen, K. K., Bigler, M., Clausen, H. B., Dahl-Jensen, D., Davies, S. M., et al. (2008). A 60,000 year Greenland stratigraphic ice core chronology. *Climate of the Past*, *4*, 47–57.

Takahashi, T., Sutherland, S. C., Sweeney, C., Poisson, A., Metzl, N., Tilbrook, B., et al. (2002). Global sea-air CO_2 flux based on climatological surface ocean pCO_2, and seasonal biological amd temperature effects. *Deep-Sea Research II*, *49*, 1601–1622.

Tessin, A. C., & Lund, D. C. (2013). Isotopically depleted carbon in the mid-depth South Atlantic during the last deglaciation. *Paleoceanography*, *28*, 296–306.

Thiagarajan, N., Subhas, A. V., Southon, J. R., Eiler, J. M., & Adkins, J. F. (2014). Abrupt pre-Bolling-Allerod warming and circulation changes in the deep ocean. *Nature*, *511*, 75–78.

Thornalley, D. J. R., Barker, S., Broecker, W., Elderfield, H., & McCave, I. N. (2011). The deglacial evolution of North Atlantic deep convection. *Science*, *331*, 202–205.

Thornalley, D. J. R., Bauch, H. A., Gebbie, G., Guo, W., Ziegler, M., Bernasconi, S. M., et al. (2015). A warm and poorly ventilated deep Arctic Mediterranean during the last glacial period. *Science*, *349*, 706–710.

Umling, N. E., & Thunell, R. C. (2017). Synchronous deglacial thermocline and deep-water ventilation in the eastern equatorial Pacific. *Nature Communications*, *8*, 14203.

van Aken, H. (2000). The hydrography of the mid-latitude northeast Atlantic Ocean I: The deep water masses. *Deep-Sea Research I*, *47*, 757–787.

Vogel, J. S., Southon, J. R., Nelson, D. E., & Brown, T. A. (1984). Performance of catalytically condensed carbon for use in accelerator mass spectrometry. *Nuclear Instruments and Methods in Physics Research Section B: Beam Interactions with Materials and Atoms*, *5*, 289–293.

Waelbroeck, C., Lougheed, B. C., Vazquez Riveiros, N., Missiaen, L., Pedro, J., Dokken, T., et al. (2019). Consistently dated Atlantic sediment cores over the last 40 thousand years. *Scientific Data*, *6*, 165.

Waelbroeck, C., Pichat, S., Böhm, E., Lougheed, B. C., Faranda, D., Vrac, M., et al. (2018). Relative timing of precipitation and ocean circulation changes in the western equatorial Atlantic over the last 45 kyr. *Climate of the Past*, *14*, 1315–1330.

Waelbroeck, C., Skinner, L., Labeyrie, L., Duplessy, J.-C., Michel, E., Vázquez Riveiros, N., & Gherardi, J.-M. (2011). The timing of deglacial circulation changes in the Atlantic. *Paleoceanography*, *26*, PA3213.

Wolff, E., Fischer, H., & Rothlisberger, R. (2009). Glacial terminations as southern warmings without northern control. *Nature Geoscience*, *2*, 206–209. https://doi.org/10.1038/ngeo442

Yu, J., Broecker, W. S., Elderfield, H., Jin, Z., McManus, J., & Zhang, F. (2010). Loss of carbon from the deep sea since the last glacial maximum. *Science*, *330*, 1084–1087.

Yu, J., Menviel, L., Jin, Z. D., Thornalley, D. J. R., Foster, G. L., Rohling, E. J., et al. (2019). More efficient North Atlantic carbon pump during the last glacial maximum. *Nature Communications*, *10*, 2170.

Zhao, N., Marchal, O., Keigwin, L., Amrhein, D., & Gebbie, G. (2018). A synthesis of deglacial deep-sea radiocarbon records and their (In) Consistency with modern ocean ventilation. *Paleoceanography and Paleoclimatology*, *33*, 128–151.

References from the Supporting Information

Butzin, M., Köhler, P., & Lohmann, G. (2017). Marine radiocarbon reservoir age simulations for the past 50,000 years. *Geophysical Research Letters*, *44*(16), 8473–8480. https://doi.org/10.1002/2017GL074688

Ruth, U., Wagenbach, D., Steffensen, J. P., & Bigler, M. (2003). Continuous record of microparticle concentration and size distribution in the central Greenland NGRIP ice core during the last glacial period. *Journal of Geophysical Research: Atmospheres*, *108*(D3). https://doi.org/10.1029/2002JD002376

Southon, J., Noronha, A. L., Cheng, H., Edwards, R. L., & Wang, Y. (2012). A high-resolution record of atmospheric C-14 based on Hulu Cave speleothem H82. *Quaternary Science Reviews*, *33*, 32–41. https://doi.org/10.1016/j.quascirev.2011.11.022

Svensson, A., Andersen, K., Bigler, M., Clausen, H. B., Dahl-Jensen, D., Davies, S. M., et al. (2008). A 60,000 year Greenland stratigraphic ice core chronology. *Climate of the Past*, *4*, 47–57.